Earth's Future

RESEARCH ARTICLE
10.1029/2024EF004531

Special Collection:
CMIP6: Trends, Interactions, Evaluation, and Impacts

Future Climate Projections for South Florida: Improving the Accuracy of Air Temperature and Precipitation Extremes With a Hybrid Statistical Bias Correction Technique

Leila Rahimi[1], Mushfiqul Hoque[1], Ebrahim Ahmadisharaf[1], Nasrin Alamdari[1], Vasubandhu Misra[2], Ana Carolina Maran[3], Shih-Chieh Kao[4], Amir AghaKouchak[5,6], and Rocky Talchabhadel[7]

[1]Department of Civil and Environmental Engineering, Resilient Infrastructure and Disaster Response (RIDER) Center, FAMU-FSU College of Engineering, Tallahassee, FL, USA, [2]Department of Earth, Ocean and Atmospheric Science, Florida State University, Tallahassee, FL, USA, [3]South Florida Water Management District, West Palm Beach, FL, USA, [4]Oak Ridge National Laboratory, Oak Ridge, TN, USA, [5]Department of Civil and Environmental Engineering, University of California Irvine, Irvine, CA, USA, [6]United Nations University Institute for Water, Environment and Health, Hamilton, ON, Canada, [7]Department of Civil and Environmental Engineering, Jackson State University, Jackson, MS, USA

Abstract Projecting future climate variables is essential for comprehending the potential impacts on hydroclimatic hazards like floods and droughts. Evaluating these impacts is challenging due to the coarse spatial resolution of global climate models (GCMs); therefore, bias correction is widely used. Here, we applied two statistical methods—standard empirical quantile mapping (EQM) and a hybrid approach, EQM with linear correction (EQM-LIN)—to bias correct precipitation and air temperature simulated by nine GCMs. We used historical observations from 20 weather stations across South Florida to project future climate under three shared socioeconomic pathways (SSPs). Compared to the EQM, the hybrid EQM-LIN method improved R^2 of daily quantiles by up to 30% over the historical period and improved MAE up to 70% in months that contain most extreme values. Projected extreme precipitation at the weather stations showed that, compared to the EQM-LIN, the EQM method underestimates the high quantiles by up to 26% in SSP585. The projected changes in annual maximum precipitation from historical period (1985–2014) to near future (2040–2069) and far future (2070–2100) were between 2% and 16% across the study area. Projected future precipitation suggested a slight decrease during summer but an increase in fall. This, along with rising summer temperatures, suggested that South Florida can experience rapid oscillations from warmer summers and increased flooding in fall under future climate. Additionally, our comparative analyses with globally and nationally downscaled studies showed that such coarse scale studies do not represent the climatic extremes well, particularly for high quantile precipitation.

Plain Language Summary Natural hazards, such as flooding and extreme heat, can damage our infrastructure and local communities. These hazards often stem from extreme weather conditions such as heavy precipitation and hot temperatures. Global climate change is expected to affect precipitation and air temperature, leading to more extreme weather events and hazards in the future. Predicting frequency and severity of these future events is key to protect our infrastructure and communities. Climate models have been widely used to project statistics of future extremes. However, they come with uncertainties due to numerical approximations, low spatial resolutions etc. Consequently, predictions generated by these models are inherently uncertain. This paper used a new approach to improve future projections of extreme climatic events, focusing on South Florida. Our findings revealed substantial improvements in projecting future events, particularly for extreme precipitation. We also showed that nationally and globally derived simulations may not be suitable for accurately projecting heavy precipitation, but can suffice for air temperature and low/medium precipitation rates. This paper offers promising avenues for refining projections of future weather events. By enhancing our ability to anticipate upcoming weather events more accurately, we can better protect our infrastructure and communities against the challenges posed by climate change.

Key Points:

- A hybrid statistical approach to improve bias correction of GCM precipitation and air temperature simulations
- Major improvements in both climatic variables, especially extreme precipitation, using our hybrid statistical approach in South Florida
- Coarse resolution downscaled data may be insufficient for deriving high quantile precipitation at the regional scale

Supporting Information:

Supporting Information may be found in the online version of this article.

Correspondence to:

E. Ahmadisharaf,
eahmadisharaf@eng.famu.fsu.edu

Citation:

Rahimi, L., Hoque, M., Ahmadisharaf, E., Alamdari, N., Misra, V., Maran, A. C., et al. (2024). Future climate projections for South Florida: Improving the accuracy of air temperature and precipitation extremes with a hybrid statistical bias correction technique. *Earth's Future*, *12*, e2024EF004531. https://doi.org/10.1029/2024EF004531

Received 23 FEB 2024
Accepted 17 JUN 2024

Author Contributions:

Conceptualization: Leila Rahimi, Ebrahim Ahmadisharaf, Vasubandhu Misra, Ana Carolina Maran
Data curation: Mushfiqul Hoque
Formal analysis: Leila Rahimi, Mushfiqul Hoque
Methodology: Leila Rahimi, Ebrahim Ahmadisharaf, Nasrin Alamdari, Vasubandhu Misra, Shih-Chieh Kao, Amir AghaKouchak

1. Introduction

Changes in the characteristics of meteorological variables, such as precipitation and temperature, can have substantial impacts on the frequency and severity of hydroclimatic hazards such as floods, droughts and extreme

Software: Leila Rahimi, Mushfiqul Hoque
Supervision: Ebrahim Ahmadisharaf, Nasrin Alamdari
Visualization: Mushfiqul Hoque
Writing – original draft: Leila Rahimi
Writing – review & editing: Ebrahim Ahmadisharaf, Nasrin Alamdari, Vasubandhu Misra, Ana Carolina Maran, Shih-Chieh Kao, Amir AghaKouchak

heat events (Arnell & Gosling, 2015; Bates et al., 2021; Cook et al., 2018; Dai et al., 2018; Gilroy & McCuen, 2012; Mukherjee et al., 2018; O'Gorman, 2015; Schiermeier, 2018; Trenberth, 2011). These hazards pose threats to the well-being of communities, the safety of infrastructure and the health of ecosystem (Hallegatte et al., 2013; Mayou et al., 2024; Naumann et al., 2021; Wing et al., 2018). Projecting potential changes in meteorological variables and incorporating them into hazard assessments as well as in the design, planning and operation of water infrastructures (e.g., gated spillways and pumps), can help ensure adequate hydraulic protection to safeguard against these threats.

To project future climate conditions, global climate models (GCMs) can be used as physics-based predictive tools. However, given the coarse spatial resolution (∼100–∼500 km), downscaling and bias correction are required before they can be used for regional- and local-scale applications (Mendoza Paz & Willems, 2022). In addition, an ensemble of skillful GCMs should be used together to better capture the inherent uncertainty and increase the reliability of future projections. To achieve these goals, either dynamical or statistical approach can be used. Treating the GCM outputs as the boundary conditions, dynamical downscaling uses a regional climate model (RCM) to refine the projections of GCMs into finer spatial resolution (Shamir et al., 2019). However, it needs extensive computational resources and is not ideal to support ensemble GCM downscaling (Walton et al., 2020; Xu et al., 2021; L. Zhang et al., 2020). Statistical downscaling (SD), on the other hand, uses the empirical relationship between historical observation and baseline GCM simulation as a basis for downscaling and bias correction (Shamir et al., 2019). However, SD techniques can only be applied when there are sufficiently long historical observations. These techniques also rely on the basic assumption that the empirical relationship does not change significantly in the future. Despite the limitations, SD is widely popular due to the computational advantages (Araya-Osses et al., 2020; Carpenter & Georgakakos, 2001; Jebeile et al., 2020; Nourani et al., 2019). In particular, it is more feasible to employ SD across a range of GCMs and climate scenarios to support ensemble-based impact assessments. Additionally, dynamical downscaling methods are also subject to limitations. Misra et al. (2019) showed that the hydroclimate of Florida is strongly associated with the seasonal evolution of Atlantic Ocean and Gulf of Mexico, which are rather poorly resolved in the GCMs. For example, shallow waters of the West Florida Shelf are not represented in most GCMs. Srivastava et al. (2021) showed that dynamically downscaled RCMs generally underestimate the magnitude of monthly precipitation and the frequency of extreme rainfall in summer across Florida. Lim et al. (2007) found that statistically downscaled time series exhibit seasonal variability much closer to the observations. We, therefore, focused on SD methods in this study. For these reasons, we only focused on SD methods in this study.

The main assumption in SD methods is *informative assumption*, which refers to the relationship between predictors and a predictand, a critical point for developing these methods (Fu et al., 2018; Sachindra et al., 2018; Yang et al., 2019). Choosing predictors should be based on the physical processes behind the changes in the predictand. For instance, precipitation as a predictand, in the physical process, responds to large-scale atmospheric circulation and thermodynamic laws (Emori & Brown, 2005; Kröner et al., 2016; Santos et al., 2016), in which sea level pressure, geopotential height, relative humidity and dew point temperature are example predictors (Maraun & Widmann, 2017; Van Uytven et al., 2020). Another key assumption in the SD methods is *perfect prognosis assumption*, which is evaluated with bias correction analyses. This assumption supposes that predictors are well represented by the GCMs (Legasa et al., 2023). The bias of predictors stems from other issues, like the climate model spatial resolution (Davini et al., 2017) and internal variability of predictors (Broucke et al., 2018). *Stationarity assumption*, which assumes a relationship between a predictand and predictors in historical observations, is useful for projections under climate change (Lanzante et al., 2018; Wang et al., 2018). The predictand sensitivity to greenhouse gas scenarios is explained by the selection of predictors (Schoof, 2013; Uytven & Willems, 2018). In addition to these general assumptions, each SD method has its own structural assumptions. The reader is referred to the literature (e.g., Hewitson et al., 2014; Maraun & Widmann, 2017; Sunyer et al., 2015) for more details about SD methods for precipitation. The main classes of SD include weather generators (Keller et al., 2017), analogs and weather typing (Bettolli, 2021; Camus et al., 2014), and regression models (Hessami et al., 2008; Schoof & Pryor, 2001; Shen et al., 2021). However, objective evaluations on the accuracy of SD methods remain an open challenge.

It is commonly recognized that the GCM-based climate projections are highly uncertain, particularly with regards to precipitation and its corresponding extremes (Stocker et al., 2013). Main sources of uncertainty in climate projections include model uncertainty and intrinsic climate variability as well as future greenhouse gas emission scenarios (Latif, 2011; Xu et al., 2021). A vast majority of bias correction approaches attempt to alter the mean,

variance and quantiles of a given meteorological variable's distribution (Fauzi et al., 2020; Mishra et al., 2020; Sangelantoni et al., 2019). Here, we focused on *empirical quantile mapping (EQM)*, a popular bias correction method, and a specific implementation of quantile mapping, which relies on empirical estimates of the quantiles from observed data and model simulations. In the EQM, the output at a daily timescale is slightly different from the quantile of observed data in extreme values, presenting distortion in the estimation of extreme variables (Kim et al., 2021; Themeßl et al., 2012). Past research (e.g., Themeßl et al., 2011) showed that the EQM outperforms other downscaling and bias correction methods, although it contains limitations to the bias correction of extreme variables. To improve the accuracy of downscaling and bias correction, especially for extreme values, we demonstrated the applicability of a hybrid approach named EQM with linear correction (EQM-LIN) (Holthuijzen et al., 2022).

Our main objective was to project changes in future precipitation and air temperature in South Florida—a complex region with a history of climate-related issues (e.g., flooding)—through improving the bias correction process for climatic extremes. The specific objectives were to: (a) compare the performance of EQM-LIN against conventional EQM in bias correcting the climatic variables of interest and future climatic extremes; (b) quantify future changes in precipitation as well as minimum and maximum daily temperature through year 2100; (c) identify suitable GCMs for projecting these climate variables in the study area; and (d) translate future changes in terms of number of dry and wet days as well as temporal trends. The unique aspect of this paper was evaluating a hybrid statistical approach (EQM-LIN) to increase the accuracy of bias correction of extreme climatic variables. Nine GCMs from the latest Coupled Model Intercomparison Project Phase 6 (CMIP6) (Eyring et al., 2016) across three shared socioeconomic pathways (SSPs)—SSP126, SSP245, and SSP585—were bias corrected by both EQM and EQM-LIN methods.

2. Study Area

Our geographic focus was South Florida, the jurisdiction of the South Florida Water Management District (SFWMD). The region comprises a highly regulated water system, with numerous regulating infrastructures such as gated spillways and pumps. It also includes large population centers like Miami, West Palm Beach, Orlando, and Naples, as well as valuable climate-dependent ecosystems, such as Everglades National Park. The landscape in the study region is diverse, with large population centers concentrated in the southeastern part of the study area. Notably, Miami is consistently ranked as one of the most vulnerable cities to coastal flooding (Kulp & Strauss, 2017). Agricultural areas (e.g., Everglades agricultural area) are located in the northern part of the study region. The remaining areas are predominantly occupied by marshes that are ecologically valuable. All these elements may face threats from climate change. South Florida has a subtropical climate and covers a drainage area of ∼18,000 km^2.

In terms of inter-annual climate variability, South Florida experiences two primary seasons: wet (June–October) and dry (November–May). The greater region, Southeastern US, is significantly influenced by the fluctuation of sea surface temperatures attributed to the El Niño/La Niña cycle. This cycle plays a crucial role in driving year-to-year climate variability across these areas. The water management system in South Florida is governed by the operation of ∼1,300 water control infrastructures (e.g., gated spillways) a network of ∼2,600 km of canals and levees, 66 pump stations, and multiple artificial reservoirs (Volk et al., 2017). Many of these infrastructures were designed and constructed before 1980 and now face climate conditions that differ from their original design specifications (Y. Zhang, 2012).

Climate change has led to abnormal wet weather conditions, thereby affecting the hydrologic regime. Elevated surface water levels increase flood risks and pose threats to valuable ecosystems in the region. South Florida has experienced climatic extremes, such as Hurricane Ian in 2022 and recent heavy rainfalls in 2023 (around Ft. Lauderdale) and 2024 (around Miami), which are expected to become more frequent and intense due to climate change. To meet water resources management goals and ensure the functionality and safety of man-made water infrastructures, strategies must consider potential future climate changes. The Comprehensive Everglades Restoration Plan (National Academies of Sciences & Medicine, 2022), the largest ecosystem restoration program in South Florida, was authorized in 2000 under Water Resources Development Act. Its purpose is to protect the South Florida ecosystem while achieving other management objectives, such as flood control and water supply. However, climate change is still not adequately considered in this plan.

10.1029/2024EF004531

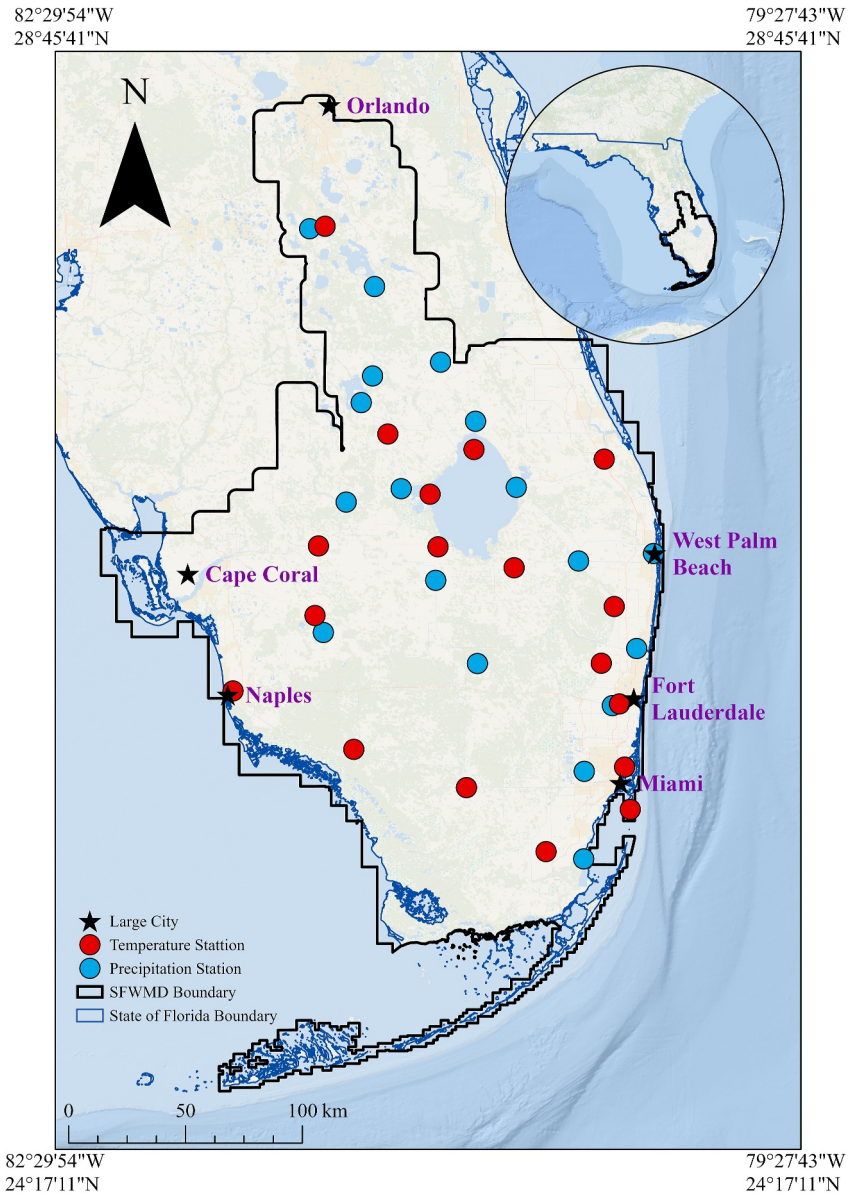

Figure 1. Study area, large cities and weather stations. SFWMD: South Florida Water Management District.

3. Data Acquisition

Climate data were acquired from 20 precipitation and 18 air temperature stations (Figure 1), which were selected based on the data completeness and the historical period of interest (1985–2014). The daily precipitation data were collected from SFWMD's DBHYDRO and the daily maximum and minimum temperature were collected from National Oceanic and Atmospheric Administration's (NOAA's) National Center for Environmental Information (NCEI). Nine CMIP6 GCMs were selected for our analyses based on previous studies performed in the entire US (Akinsanola et al., 2020; Almazroui et al., 2021; Srivastava et al., 2020; Xu et al., 2021). Among these models, six were used by a recent national scale study led by the Oak Ridge National Laboratory (ORNL) (Ashfaq et al., 2022; Kao et al., 2022; Rastogi et al., 2022). In addition to these, we used three other GCMs: Community Earth System Model 2 (CESM2) and two that were used in the study of Bayissa et al. (2021) for South Florida. Table 1 lists these models and their horizontal resolution. We analyzed historical conditions and three future climate scenarios, SSP126, SSP245, and SSP585. These scenarios differ in terms of future emissions of greenhouse gas, population growth, and pertinent policy.

Table 1
Global Climate Models (GCMs) Explored in This Paper

Developing institute	GCM	Horizontal resolution	Reference
Commonwealth Scientific and Industrial Research Organization & Australian Research Council Centre of Excellence for Climate System Science	ACCESS-CM2	1.9° × 1.3°	Dix et al. (2019)
Beijing Climate Center	BCC-CSM2-MR	1.1° × 1.1°	Wu et al. (2018)
Canadian Centre for Climate Modeling and Analysis	CanESM5	2.8° × 2.8°	Swart et al. (2019)
National Center for Meteorological Research, Météo-France and CNRS	CNRM-ESM2-1	1.4° × 1.4°	Seferian (2018)
European community Earth-System Model	EC-Earth3-Veg	0.7° × 0.7°	EC-Earth Consortium (EC-Earth) (2019)
Max Plank Institute	MPI-ESMI-2-LR	1.9° × 1.9°	Mauritsen et al. (2019)
Meteorological Research Institute	MRI-ESM2-0	1.1° × 1.1°	Yukimoto et al. (2019)
Norwegian Climate Center	NorESM2-MM	0.9° × 1.3°	Seland et al. (2020)
National Center for Atmospheric Research, USA	CESM2	2.8° × 2.8°	Danabasoglu (2019)

4. Methodology

The CMIP6 archive contains more than 40 latest GCMs from several modeling groups across the world with a variety of experiments (Eyring et al., 2016). These models can be utilized for effective climate sensitivity analyses and future projections of meteorological variables based on different emission scenarios, represented by SSPs (McBride et al., 2021). We statistically bias corrected precipitation as well as maximum and minimum daily air temperature from the nine GCMs (Table 1), against meteorological measurements at the weather stations across the study area (Figure 1) via both EQM and EQM-LIN methods. The period of 1985–2014 represents historical conditions, while 2015–2100 represents future conditions; we further split the future into two periods of 2040–2069 as near future and 2070–2100 as far future. We also derived the characteristics of extremes and evaluated the performance of the bias correction for the nine GCMs using statistical tests. A schematic view of our methodology is presented in Figure 2.

4.1. Bias Correction

Quantile mapping uses a transfer function (TF) to map quantiles of the climate model outputs to those of observations (Boé et al., 2007), thereby attempting to solve the following equation:

$$x_0 = F_0^{-1}[F_m(x_m)] \quad (1)$$

where o, m, and F are related to observed and modeled variables and their cumulative distributions, respectively (Boé et al., 2007; Panofsky, 1968; Themeßl et al., 2011, 2012). TF can be parametric or non-parametric. Among various methods (Themeßl et al., 2011, 2012)—EQM—a specific implementation of quantile mapping, can provide a non-parametric approach for distribution mapping. EQM does not require parametric distributional

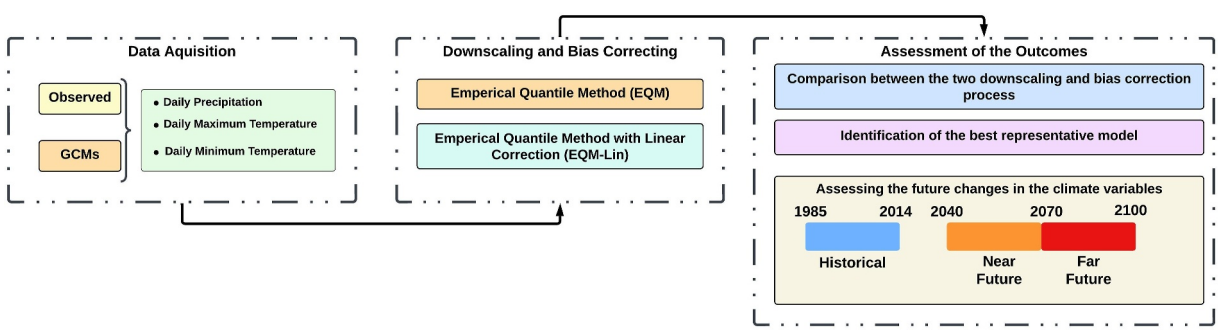

Figure 2. Schematic view of the methodology.

assumptions and offers flexibility in accordance with variability of observed and modeled variables (Boé et al., 2007).

4.1.1. Empirical Quantile Mapping Method

EQM can preserve statistical parameters like mean, standard deviation, and higher-order distributional moments that describe both data sets of observed and bias corrected variables (Gudmundsson et al., 2012; Themeßl et al., 2011). When deriving empirical cumulative distribution functions (ECDFs), if the train values that are used for estimating the ECDF are lower than those projected by climate models (i.e., model outputs), the highest quantile in the training set is employed to correct the model value (Gudmundsson et al., 2012). Suppose t as a daily timescale window for meteorological variables and $ecdf$ as an ECDF. EQM is applied to a given location i to bias correct a time series using the following steps (Themeßl et al., 2012):

$$\begin{aligned} X_{t,i}^{cor} &= X_{t,i}^{row} + CF_{t,i} \\ CF_{t,i} &= ecdf_{doy,i}^{obs,cal^{-1}}(P_{t,i}) - ecdf_{doy,i}^{\mathrm{mod},cal^{-1}}(P_{t,i}) \\ p_{t,i} &= ecdf_{doy,i}^{\mathrm{mod},cal}(X_{t,i}^{row}) \end{aligned} \tag{2}$$

These steps are categorized as a non-parametric approach (free-parametric), assuming the same parameter for the predictor and predictand. CF (Equation 2), a correction function, represents the remnant of the difference between the inverse ECDF (e.g., $ecdf^{-1}$) of the observed and modeled meteorological value on a specific day of a given year (doy). X^{row} presents a raw climate model output with the probability of P (e.g., corresponding $ecdf$ in the calibration period, in which data is divided into two sections of the train and test). The corrected value can be finally derived by the TF ($ecdfs\ invers$) using:

$$X_{t,i}^{cor} = ecdf_{t,i}^{obs,cal^{-1}}\left[ecdf_{t,i}^{\mathrm{mod},cal}(X_{t,i}^{row})\right] \tag{3}$$

where $X_{t,i}^{cor}$ is the bias corrected future projection at time t and location i. We used the qmap package (version:1.0–4) in R (Gudmundsson et al., 2012) to perform the bias correction processes. We also separated the meteorological data based on wet and dry seasons to account for the seasonality of precipitation and air temperature across the study area in our bias correction. If ECDF of the observed (e.g., $ecdf^{obs,cal}$) dry day is less than its counterpart in the model (e.g., $ecdf^{\mathrm{mod},cal}$), a frequency adaptation is needed. However, this is not the case as many climate models overestimate "drizzle" events (Gutowski et al., 2003; Zhou et al., 2022). In some cases when the model tends to summer drying (Mearns et al., 2013), frequency adaptation helps avoid the bias correction approach mapping a dry day to wet. To bias correct using frequency adaptation, ΔP_0 as a fraction of a dry day of a given year with the probability of zero (P_0), are corrected randomly using linear interpolation (for more details, see Themeßl et al. (2012)).

$$\Delta P_0 = \frac{\left[ecdf_{doy,i}^{\mathrm{mod},cal}(0) - ecdf_{doy,i}^{obs,cal}(0)\right]}{ecdf_{doy,i}^{\mathrm{mod},cal}(0)} \tag{4}$$

The correction using the linear interpolation between no precipitation and the amount of $ecdf_{i}^{obs,cal^{-1}}\left[ecdf_{t}^{\mathrm{mod},cal}(0)\right]$ removes the wet bias.

Here, quantile mapping using frequency adaptation was utilized to remove this bias for both daily precipitation and air temperature. The ECDF of dry days was set to zero, in which the threshold equals $1.0_{\frac{mm}{day}}$, (Gudmundsson et al., 2012; Polade et al., 2014) supposed to distinguish between wet and dry days.

The outputs of the bias correction approach using the EQM are bias corrected values that are employed for local scale applications. Comparisons between the coarse climate variables (simulated via GCMs and RCMs) and finer meteorological variables at a local scale for a historical period, as the control period, can help derive the relationship between the climate model outputs and observations, thereby revealing the suitability for future climate projections.

4.1.2. Limitations of Empirical Quantile Mapping

While EQM is widely popular, it has several limitations. For instance, EQM is very sensitive to the selection of a training period, and can also overfit extreme values (i.e., tail of a distribution) (Holthuijzen et al., 2021; Lafon et al., 2013). Although transform functions can be interpolated using linear interpolation or other techniques, it cannot be easily generalized to high quantiles that are outside the range of training samples. This is common for future climate projections. In particular, overfitting may distort the time series of future meteorological variables and exaggerates the trends of extreme events (Grillakis et al., 2017; Tani & Gobiet, 2019).

Bias correction via the EQM method is based on empirical percentiles, utilizing the ECDF of the observations and GCM outputs. This constrains an assumption, if the climate observations in the train window (note that the data in the bias correction process is divided into two sections of train and test) are less than the projected values, the largest future projected values are bias corrected using the highest quantile of the train window. A pivotal assumption here is that both high quantiles during the historical and future periods have the same bias. This assumption can lead to poor projections of the extreme values. Additionally, the equality of the fraction of wet days between the modeled (future) and observed (historical) values need a threshold selection; wet days in the model with values less than $1.0\,\frac{mm}{day}$ are set to zero (Boé et al., 2007; Mendoza Paz & Willems, 2022).

4.1.3. Linear Correction Within Empirical Quantile Mapping for Extremes (EQM-LIN)

To overcome these limitations and increase the stability of the TF on high quantiles, a hybrid EQM-LIN method is used here. This method contains both a non-parametric EQM approach to bias correct lower quantiles, and a robust linear correction for extreme values in upper quantiles (Holthuijzen et al., 2022). To find an optimal quantile threshold to implement both methods, we tested different quantiles. The results suggested that the best bias correction performance (minimum error) can be reached by using 0.05 and 0.95 as the lower and upper limit thresholds. Therefore, the 5th and 95th percentiles were used as the threshold value (*TH*). Values lower than the *TH* in the lower tail and those larger than *TH* in the upper tail were corrected by EQM-LIN:

$$X_{t,i}^{cor} = \begin{cases} \mathrm{ecdf}_{\mathrm{obs}}^{-1}\left[\mathrm{ecdf}_{\mathrm{mod}}\left(x_{\mathrm{mod},t}\right)\right] & x_{\mathrm{mod},t} < T \\ x_{\mathrm{mod},t} + \delta & x_{\mathrm{mod},t} \geq T \end{cases} \tag{5}$$

where, T is a precipitation value in mm and δ is a constant value at extremes. While the aim of TFs in EQM and EQM-LIN is to correct the model outputs to near perfect, the TF in EQM results in overfitting that may not generalize the future modeled data. This can lead to instability of the TF at higher quantiles. To solve the linear portion of TF($X_{t,i}^{cor} = x_{\mathrm{mod},t} + \delta$) for $x_{\mathrm{mod},t} \geq T$, slope and intersect are 1 and δ, respectively. T is considered as a threshold value, in which each observed and modeled data is divided into two portions, values smaller and greater than T, which can have an exceedance probability between 0 and 1. To minimize the mean absolute error (MAE) between the modeled and observed data, we chose T as a quantile, ranging from 60th to 95th percentiles to identify the optimal T. For more details about this approach, the reader is referred to (Boé et al., 2007; Holthuijzen et al., 2022). The standard procedure in bias correction algorithms is that the GCM outputs are compared only against one historical time series (Rastogi et al., 2022). To evaluate the efficiency of the EQM-LIN and EQM for the bias correction, 5-fold cross-validation was utilized (Holthuijzen et al., 2022). We divided the historical data into two sections: training and validation. To minimize MAE between the modeled and observed data, we selected T as a quantile ranging from the 60th to the 95th percentile to determine the optimal value of T. We conducted 5-fold cross-validation for each 0.01 step from 0.60 to 0.95 to identify the most suitable value for T.

4.2. Evaluation of the Bias Correction Performance

We used in situ observations from weather stations for the bias correction. In both EQM and EQM-LIN, the TFs for daily projections were constructed month by month (Holthuijzen et al., 2022; Piani et al., 2010; Themeßl et al., 2011); that is, 12-month-specific TFs were constructed for each method. Equation 3 was used, in which after determining the inverse ECDF of the observations, the raw GCM output was transferred in either method to arrive at the bias corrected values. This procedure, continued month-by-month to find the optimal TF in each month, considering 10,000 estimated quantiles using the qmap package in R (Gudmundsson et al., 2012).

The performance of the bias correction approach was evaluated based on comparative analyses between ECDFs of the observed and projected variables by the GCMs. To evaluate the variance (variability), distribution, and median of the bias corrected data (Han & Ines, 2017; Song et al., 2020), three statistical tests—Levene's test (to check the equality of variances between two samples; Levene, 1960), Kolmogorov-Smirnov test (to test the null hypothesis that two samples come from the same distribution or not; Massey, 1951) and non-parametric Wilcoxon rank sum test (to assess the difference of population mean ranks between two samples; Wilcoxon, 1945)—were performed to determine the statistically significant differences between the ECDFs of observed and modeled meteorological variables using the best GCMs. To compare the performance of EQM and EQM-LIN, three statistical measures—MAE, root mean square error (RMSE), and coefficient of determination (R^2)—between the estimated quantiles of observed and bias corrected variables from their ECDF were calculated (Gudmundsson et al., 2012). The best GCM refers to the closest downscaled GCM output to the observations according to the statistical measures and quantile-quantile (QQ) plots. The best GCM was then used for the future projections.

4.3. Future Projections

Three SSPs—SSP126 (low), SSP245 (median) and SSP585 (high)—were studied. Bias correction of daily precipitation as well as maximum and minimum air temperature was performed at each weather station under all three SSPs. For temporal trend analyses, the Mann-Kendall test (Aditya et al., 2021) was performed for the best GCM at each weather station. Also, using the projected precipitation, the number of wet and dry days was calculated and presented as annual values. To avoid the drizzling problem, a minimum precipitation threshold of $1.0\,\frac{mm}{day}$ was used; that is, if the bias corrected precipitation is less than $1.0\,\frac{mm}{day}$, the day is considered dry (Polade et al., 2014).

5. Results and Discussion

5.1. GCM Evaluation and Bias Correction

After implementing both bias correcting approaches (EQM and EQM-LIN) on the three meteorological variables —precipitation, maximum and minimum air temperature—over the historical period (1985–2014) at each weather station, the characteristics of ECDFs and quantiles of the observed and bias-corrected values were compared. Overall, in the historical period, the application of EQM-LIN on precipitation as well as maximum and minimum air temperature showed that this method outperforms EQM in terms of MAE and RMSE by 30% and R^2 by up to 5% (Table S1 in Supporting Information S2). These criteria present improvements by the EQM-LIN for daily values over the historical period, but the performance for month-by-month daily values was much better than that observed over the historical period, especially in the months that contain more extreme values (more discussions later in Section 5.2). After bias correcting the nine GCMs, the results showed that BCC-CSM2-MR outperforms the other models at the majority of stations (Figure 3). For these reasons, we only provided the results of the future projections using this method (EQM-LIN) and best GCMs (Figure 3) at each weather station.

Figure S1 in Supporting Information S1 summarizes the results of the three statistical tests—Wilcoxon rank-sum, Levene's test, and Kolmogorov-Smirnov—for the statistical significance of the variability in the distributions of observed and projected daily precipitation as well as maximum and minimum air temperature. The results of these tests indicated the similarity and dissimilarity of the daily observed and bias corrected precipitation and air temperature (minimum and maximum) for the best GCM at each weather station. Leven's test rejected the null hypothesis at the majority of the stations (95% confidence level), suggesting that there is a dissimilarity in the two sample data (historical observations vs. bias corrected values). This rejection might be because of the sensitivity of the Leven's test to sample size, especially in large sample sizes. These results are consistent with Song et al. (2020) for Florida, which Leven's test was also rejected at most of the weather stations. The mean and distribution of the two data sets (observed and bias corrected) were found to be similar based on the Wilcoxon rank sum test and Kolmogorov-Smirnov tests though (95% confidence level).

5.2. Performance of Empirical Quantile Mapping Method With Linear Correction (EQM-LIN)

The best GCM at each weather station was determined according to MAE, RMSE, and R^2 (Table S1 in Supporting Information S2) and comparisons between the performance of EQM and EQM-LIN in quantiles of different daily climate variables using various GCMs. The BCC-CSM2-MR model at the Miami station demonstrated superior

10.1029/2024EF004531

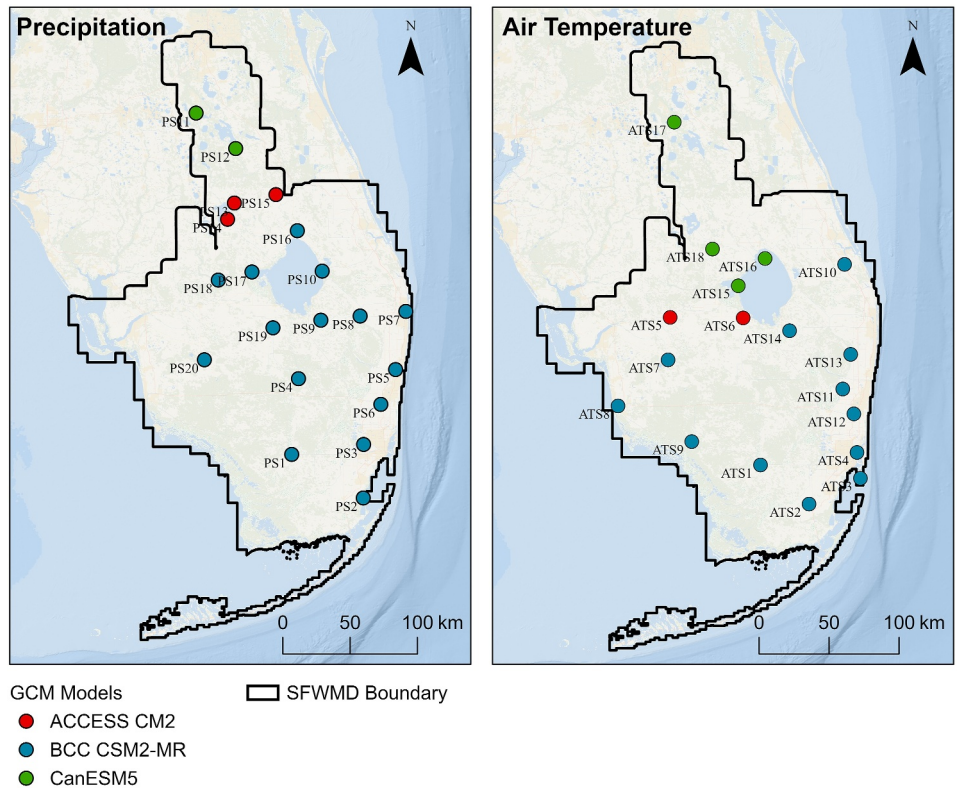

Figure 3. The best performed global climate models (GCMs) at each weather station for: (left) precipitation, and (right) maximum and minimum air temperature, across the study area.

performance according to the statistical measures, surpassing even the top-performing GCMs at the other weather stations. Consequently, this station was chosen as the representative station for conciseness in the remainder of the paper for illustration purposes. Figure 4 shows the QQ plots by applying EQM and EQM-LIN methods to both daily precipitation and maximum air temperature in the months with greatest improvements based on MAE, RMSE and R^2 (Table S2 in Supporting Information S2) at Miami station. The improvement of the bias correction after applying the linear correction (EQM-LIN) was up to 27% in R^2 and up to 70% in MAE for precipitation, and 14% (R^2) and 47% (MAE) for maximum temperature (Table S2 in Supporting Information S2). These plots show how EQM-LIN improves the performance of the bias correction (for quantiles greater than 95th percentile) and yields more similarity between the ECDFs of the observed and bias corrected values.

Our comparative analyses on the quantiles of daily precipitation (using QQ plots) at the Miami weather station showed that EQM-LIN generally outperforms the bias corrected values by other CMIP6 studies: NASA global study (downscaled data at 25 km grid spacing; Thrasher et al., 2022) and the ORNL national scale (downscaled data at 4 km grid spacing, Kao et al., 2022). The differences were particularly substantial on high quantiles of precipitation. These comparisons suggested that using such downscaled data sets can underestimate extreme values, particularly for high quantiles of precipitation. The differences can be explained by the use of different bias correction approaches and observations like Daymet that are not in situ like those used in our study. In fact, we found that the Daymet daily data set, which was used in the downscaling by ORNL (Kao et al., 2022), tends to underestimate the observed data, particularly in precipitation time series. These comparisons are illustrated in Figure 5 and Figure S3 in Supporting Information S1.

Figure 5 and Figure S3 in Supporting Information S1 present QQ plots for EQM-LIN, EQM, Thrasher et al. (2022), and Kao et al. (2022) data alongside the observations. Additional comparisons on the performance of our two bias correction approaches and the downscaled data of NASA and ORNL are provided in Figures S2 and S4 of the Supporting Information S1 month-by-month as QQ plots. The results showed that EQM-LIN generally outperformed the other bias corrected studies that were done at national and global scales.

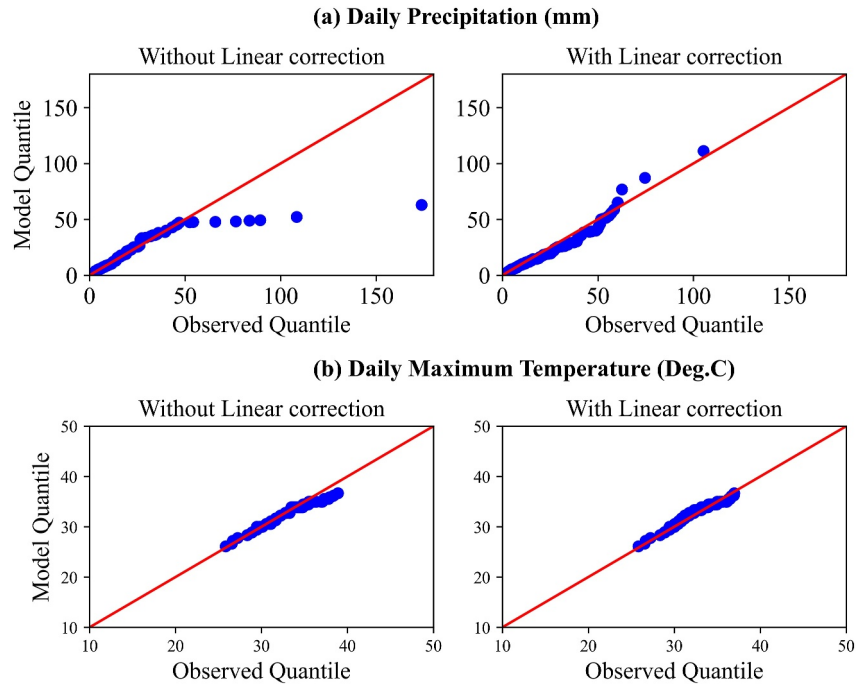

Figure 4. Quantile-Quantile plots between: (a) daily precipitation (mm) in the month of May, and (b) daily maximum temperature (°C) in the month of August (containing the highest value) at Miami weather station (the representative station with greatest improvement in the bias correction via the EQM-LIN method) using the BCC-CSM2-MR (the best performing global climate model (GCMs) among the nine GCMs evaluated in this study). (left): Empirical quantile mapping (EQM); and (right) EQM with linear correction (EQM-LIN) bias correcting approach.

5.3. Projecting Future Precipitation and Air Temperature

Figures 6 and 7 and Figures S5–S8 in Supporting Information S1 show the comparison of the ECDFs of maximum daily precipitation at the representative weather station (Miami) by applying EQM and EQM-LIN methods using the best identified GCMs in near future (2040–2069) and far future (2070–2100). Compared to EQM-LIN, EQM underestimated the extreme precipitation in the future climate scenarios. The figures emphasize the advantage of EQM-LIN in projecting the extreme precipitation, particularly in the upper tail. At most weather months, the greatest difference between EQM and EQM-LIN quantile were <26% and <20% for near future under SSP585, respectively. This deference was less for the other two SSPs. The major underestimation of extreme precipitation suggested that, the standard EQM method can be misleading in projecting heavy precipitation.

Unlike precipitation, the difference between the two bias correction methods in air temperature was small. This was expected as the improvement in bias correction was also smaller. For this reason, the results of the difference in future projections are not provided for air temperature.

Figure 8 displays shaded plots of 10-year moving averages of annual precipitation accompanied by a 95% confidence interval. These plots illustrate a declining trend in long-term annual precipitation under the three future scenarios. Similarly, Keith et al. (Ingram et al., 2013) presented negative values for annual and seasonal percent change of precipitation in the southeast US between projections for 2041–2070 and the historical period of 1971–2000. Figure 9 displays shaded plots of 10-year moving averages of annual maximum in maximum temperature and annual minimum in minimum temperature under the three SSPs. These plots reveal an overall increase in the long-term annual maximum temperature and annual minimum temperature, except for the SSP126 scenario, which shows no discernible long-term trends in annual minimum temperature. The results are partly in line with the result of the projected temperature by Almazroui et al. (2021), although they found an increase in annual mean temperature for the three future scenarios.

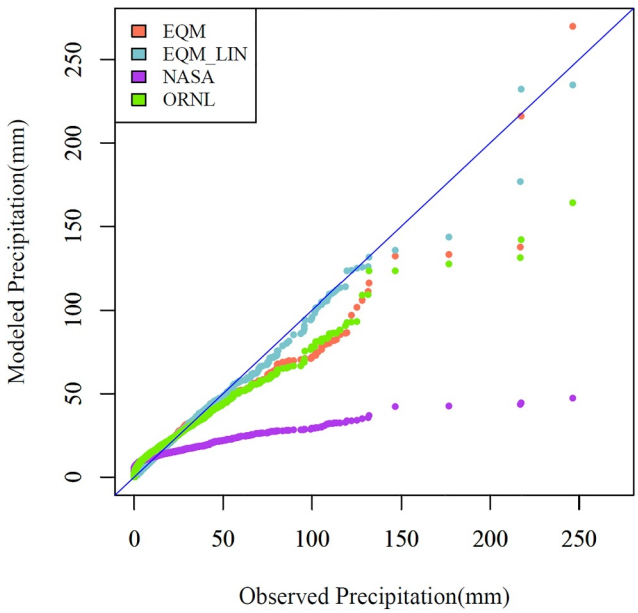

Figure 5. Quantile-Quantile plots between daily precipitation (mm) in historical period (1985–2014) using empirical quantile mapping (EQM), EQM with linear correction (EQM-LIN), NASA global study (Thrasher et al., 2022) and Oak Ridge National Laboratoy's national study (Kao et al., 2022) at Miami weather station based on BCC-CSM2-MR global climate model values.

After projecting the climate variables—precipitation as well as maximum and minimum air temperature—by EQM-LIN at each weather station via the best GCM, the mean annual maximum under three future scenarios within two periods of near future (2040–2069) and far future (2070–2100) was compared with the historical observations (1985–2014) in Figures 10 and 11. Figure 10 presents decreasing patterns in mean annual maximum of precipitation under SSP245 in both near and far future, and increasing under SSP585 in the near future and SSP126 in the far future. At the majority of weather stations, the mean values of both minimum and maximum air temperature (Figure 11) were projected to increase in both near and far future compared to the historical period. In addition, the magnitude of changes in mean annual maximum using EQM and EQM-LIN approaches presents changes between 2% and 16% (Figure 12), further highlighting that the EQM generally produces underestimated extreme values.

Figure 13 presents the comparison of observed and projected values using the best GCM and EQM-LIN (see Figure 3) in terms of monthly precipitation as well as maximum and minimum air temperature at stations close to large population centers (Miami, West Palm Beach, Orlando, and Naples) in the study area under the three SSPs. Although sample sizes of variables (observed and projected time series size) in historical (1985–2014) and future (2015–2100) periods were different, which increased the uncertainty of the comparisons, but due to the similarity of ECDFs in historical and future projected variables, this comparison was deemed acceptable.

Figures 13a–13d presents that, in general, the median of monthly precipitation in historical and future scenarios (SSP126, SSP245, and SSP585) during months around the winter (December, January, February, and March) are similar. Also, the maximum value of monthly precipitation (disregarding any outliers) stayed below $200\frac{mm}{day}$. In the majority of the four weather stations, particularly at Miami, West Palm Beach, and Naples (Figures 13a–13d) in August, there was a decline in the first and second quartiles (Q_1 and Q_2) of monthly precipitation in the future scenarios compared to the historical period. In contrast, the third quartile (Q_3) still raised. These suggested the potential for a downward shift in the magnitude of future monthly precipitation in these months, especially in the summer with the most extreme air temperature. Also, Figures 13e–13g presents an escalation in the average of maximum temperature in June, July, and August. This decrease in the monthly precipitation values can be explained by a combination of air temperature, humidity, and precipitation, which was found by Alizadeh-Choobari and Najafi (2018) and Siabi et al. (2023) that increasing temperature under climate change drives water vapor inland and decreases precipitation in coastal parts. Such a shifting may make the study area prone to droughts rather than flooding in the summer. Also, in the majority of the four stations near the large population centers, there was a rising monthly precipitation in the fall (October and November), suggesting potential increases in flooding during this season. In a broader context, the fluctuations of daily precipitation magnitude across three future scenarios exhibited greater changes compared to daily maximum and minimum air temperatures. This might arise from the erratic nature of precipitation (Siabi et al., 2023). The fluctuation was also visible in the monthly data set of precipitation and temperature.

To further assess the changes of climate variables in the study area under future scenarios, Mann-Kendall trend test was performed on different time series of precipitation and air temperature. The result of trend analyses in monthly and annual precipitation time series also confirmed the variability observed in the boxplots (Figures 13a–13d) at the four stations near large population centers. At the majority of stations, monthly precipitation presented a slightly decreasing trend in the summer (June, July, and August) and increasing trend in November and slightly decreasing trend annually (95% confidence interval). This finding was also in line with the previous studies (Butcher et al., 2023; Infanti et al., 2020; Obeysekera et al., 2017), which projected decreases in monthly precipitation during the summer in South Florida. The combination with rising temperatures in these months accentuates that the study area is projected to be prone to droughts in the summer and flooding over the fall. Ghanbari et al. (2023) found that dry and hot days are increasing in the future in the southeast US, although the

10.1029/2024EF004531

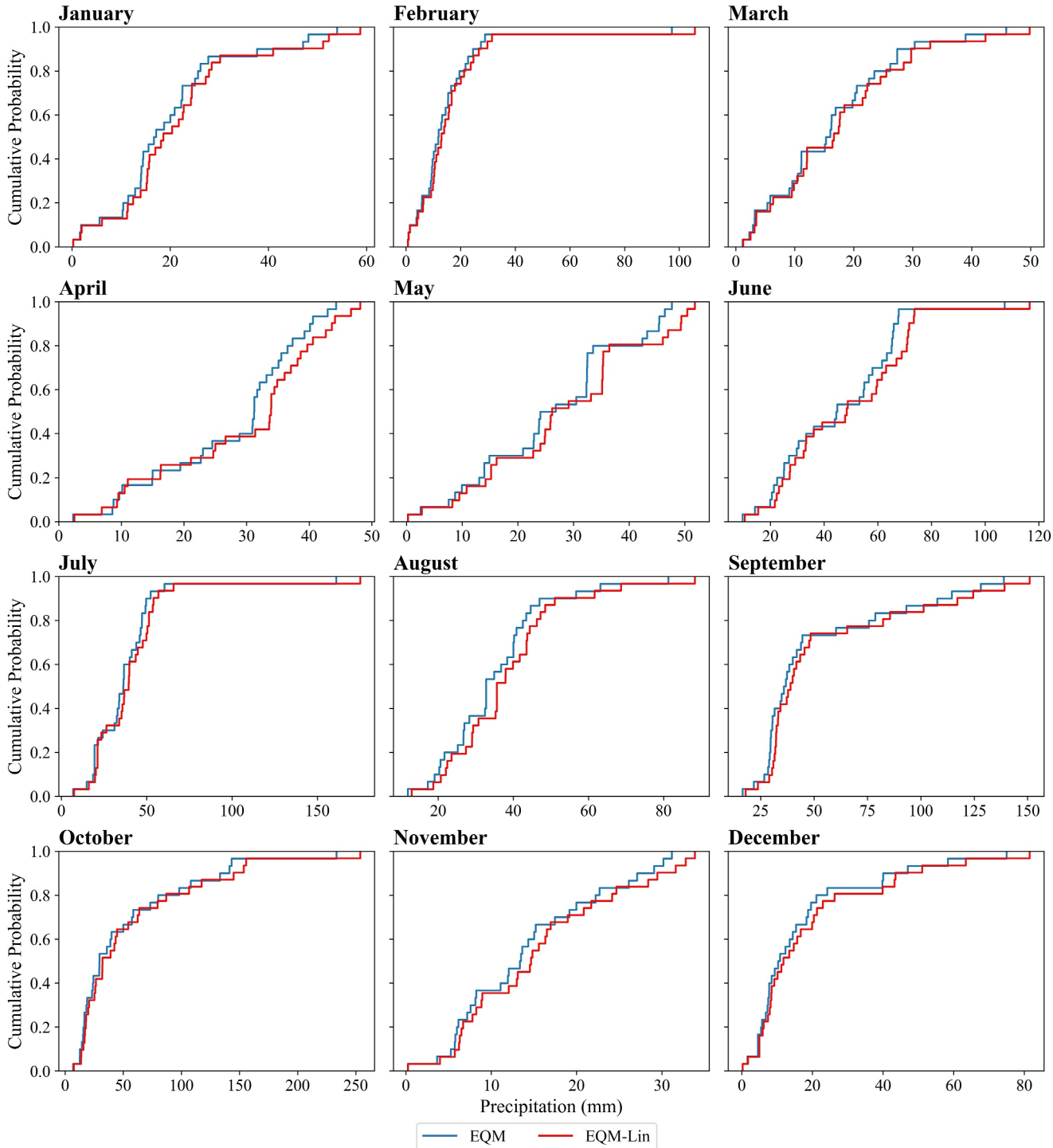

Figure 6. Empirical cumulative density functions (ECDFs) of daily maximum precipitation applying empirical quantile mapping (EQM) and EQM with linear correction (EQM-LIN) within near future (2040–2069) under SSP126 scenario at Miami weather station using the BCC-CSM2-MR global climate model outputs.

seasonality of changes was not reported. The magnitude of the most extreme daily precipitation in the future under SSP585 scenario, compared to the historical period at the four weather stations near the major cities (Miami, West Palm Beach, Orlando, and Naples), presented an upward trend in both near future (2015–2055) and far future (2056–2100). The frequency of extreme daily precipitation (exceedance of the 99th percentile) showed slight

10.1029/2024EF004531

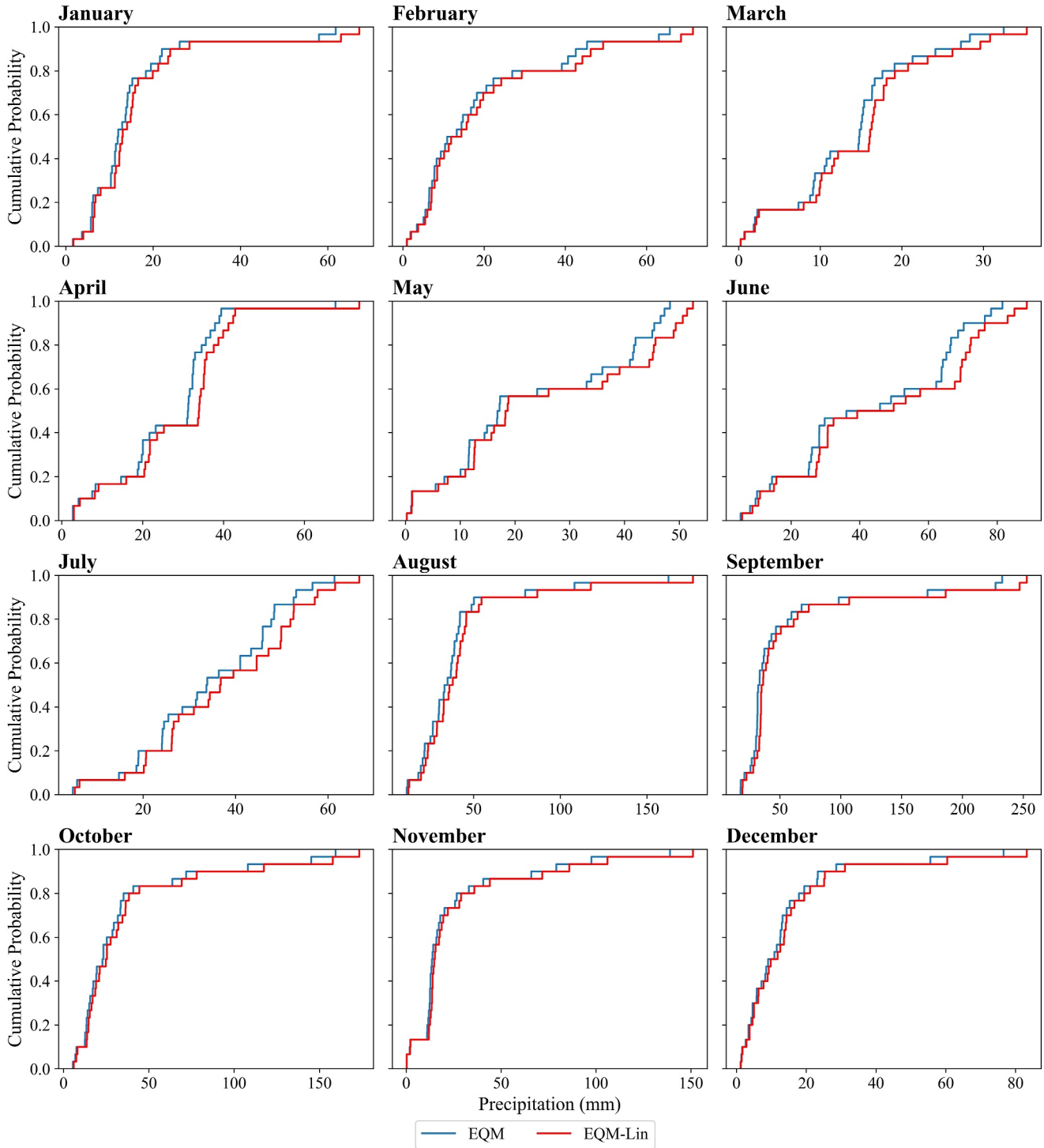

Figure 7. Empirical cumulative density functions (ECDFs) of daily maximum precipitation applying empirical quantile mapping (EQM) and EQM with linear correction (EQM-LIN) within near future (2040–2069) under SSP585 scenario at Miami weather station using the BCC-CSM2-MR global climate model outputs.

increases in the near future (2015–2055) and decreases in the far future (2056–2100) at these stations though. Irizarry-Ortiz et al. (2022) also projected a slightly upward trend in the future precipitation (2050–2089) based on bias corrected climate data sets with durations of 1, 3, and 7 days. Long-term changes in precipitation and air

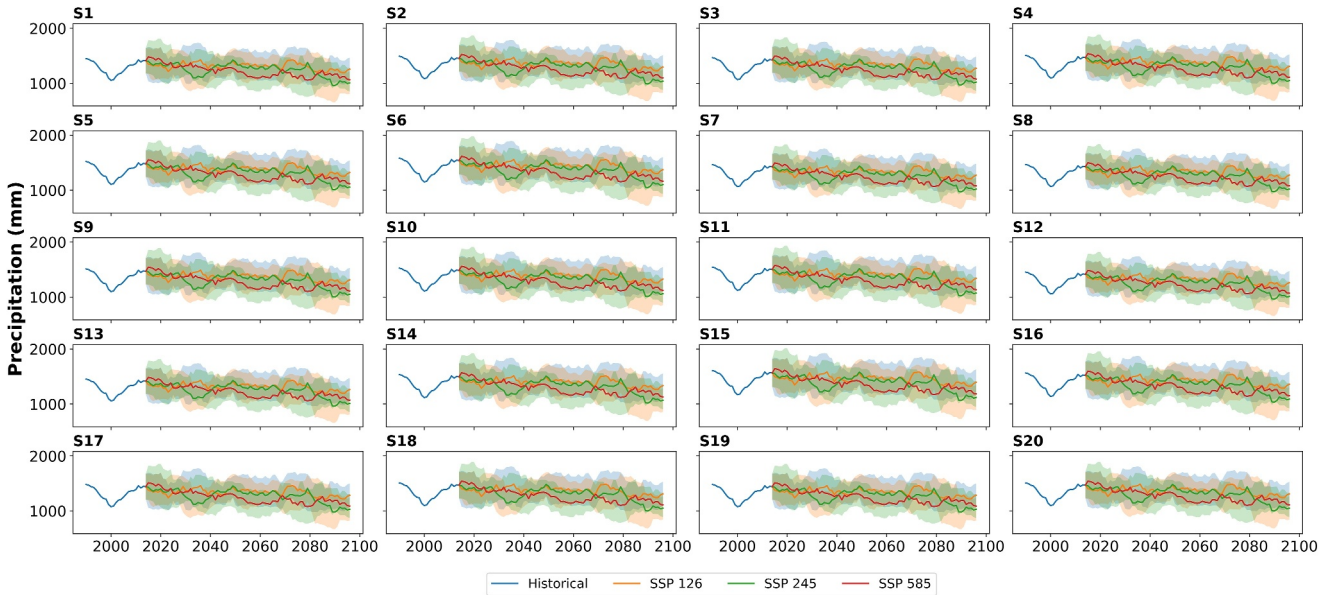

Figure 8. Shaded plots representing a 10-year moving average of annual precipitation, accompanied by 95% confidence intervals, under three future scenarios (2015–2100) using empirical quantile mapping with linear correction (EQM-LIN) and the best global climate model at each weather station (S1, S2 etc.).

temperature can have an adverse effects on the amount of water available downstream, leading to drought or flooding occurrences that have negative impacts on local communities. The findings of our study can support efforts that improve the safety of infrastructure, such as drainage systems and flood protection strategies, and resistance to droughts.

For the average annual maximum and minimum air temperature, no trend was observed in the historical data but mostly increasing trends were observed in the future scenarios (5% significant level; Figure 14). This is in line with NOAA (2022) that summarized the projection of key climate variables under the Representative Concentration Pathways (RCPs)—RCP8.5 CMIP5 scenarios—and suggested that the median air temperature is expected to increase for Southern and Central Florida based on an ensemble of CMIP5 models.

For further evaluation of future changes in the precipitation characteristics, we compared the annual number of wet and dry days under historical and future scenarios in Figure 15. We found that the number of dry days is greater than wet days in both historical and future periods, but it is projected to increase from the lowest-warming scenarios (SSP126) to the higher-warming scenarios (SSP585) at each weather station.

US Department of Agriculture (USDA, 2024) also reported that, over the recent decades, there has been a noticeable decline in summer precipitation. The majority of climate models suggested that this reduction in summer precipitation can persist in the coming years, with the most significant decreases (exceeding 10%) projected to occur in South Florida and the western states of the southeast US. USDA (2024) also projected a plausible decrease in the mean annual precipitation over the western portion of the southeast US. Florida has a specific climate pattern due to natural modes—the Atlantic Multi-decadal Oscillation (AMO), the El Niño Southern Oscillation (ENSO), and the Pacific Decadal Oscillation (PDO)—all of which significantly affect Florida's climate variability. In addition, other climate cycles, such as the solar cycle and North Atlantic Oscillation (NAO)/Arctic Oscillation (AO), have an unclear impact on Florida's climate. Winter and early spring in southeast US and Florida, are strongly influenced by ENSO. The climate in southeast US is not symmetrical between the El Niño and La Niña years, due to the climate experience of cold and wet winters in warm ENSO years, and warm and dry winters in cold ENSO (La Niña) years (Joshi & Kalra, 2021; Kirtman et al., 2017; Misra et al., 2011). Due to the frequent experience of Florida's climate to all above mentioned teleconnections, the trend analyses by the Mann-Kendall test and some statistical tests may not capture all climate conditions.

10.1029/2024EF004531

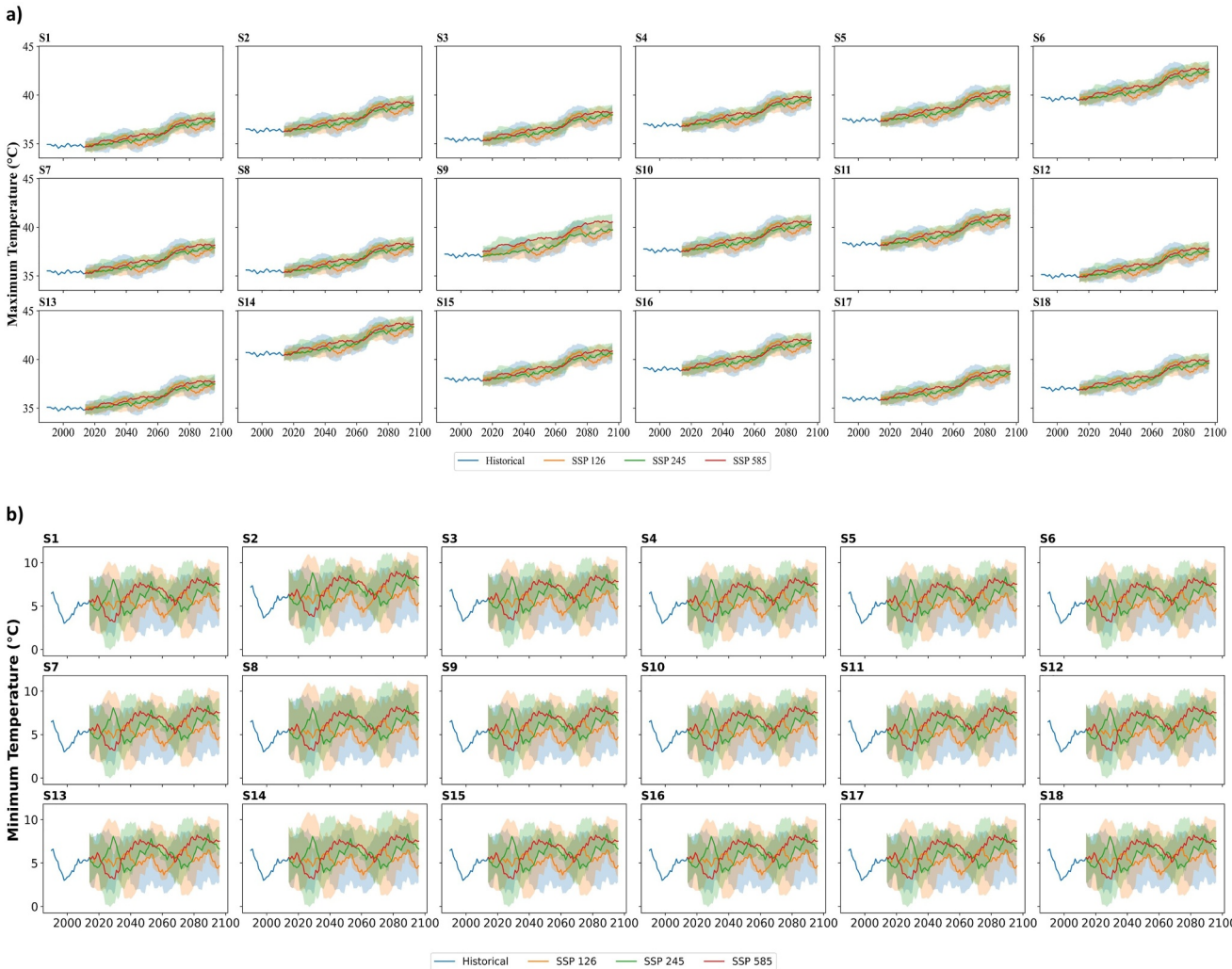

Figure 9. Shaded plots representing a 10-year moving average of: (a) annual maximum in maximum temperature and (b) annual minimum in minimum temperature, accompanied by 95% confidence intervals, under three future scenarios (2015–2100) using empirical quantile mapping with linear correction (EQM-LIN) and best global climate model at each weather station (S1, S2 etc.).

5.4. Limitations and Future Work

This paper was exclusively centered on prospective changes in precipitation and air temperature. Other meteorological variables (e.g., wind speed and evapotranspiration), which can affect the water cycle, should be studied to provide a more comprehensive picture of plausible future changes in the regional climate. We utilized about ∼20 weather stations for projecting precipitation and air temperature under future climate scenarios. A denser network of stations would result in better capturing the spatial pattern of these variables. We used 1985–2014 as the historical period for our bias correction. While this is a commonly used period for bias correcting the GCM outputs of CMIP6 scenarios, the selection of this period may affect the results of bias correction and future projections. For future analyses, if one aims to explore the influence of the selected historical period on bias correction results, multiple periods can be explored, assuming long-term observations exist.

Additionally, RCMs, which have a higher spatial resolution than GCM, should be studied in the future to evaluate their efficiency in the study area. The majority of methods for SD are implemented with the underlying presumption that the statistical correlation between GCM outputs and detailed observational data, as established under current climatic conditions, will persist even as climate changes in the future (Boé et al., 2006; Wilby et al., 1998). Dynamically downscaling techniques, which apply the outputs of RCMs, can be used to compare with our results derived by the two SD methods. The projected climate variables can be used to study the impacts

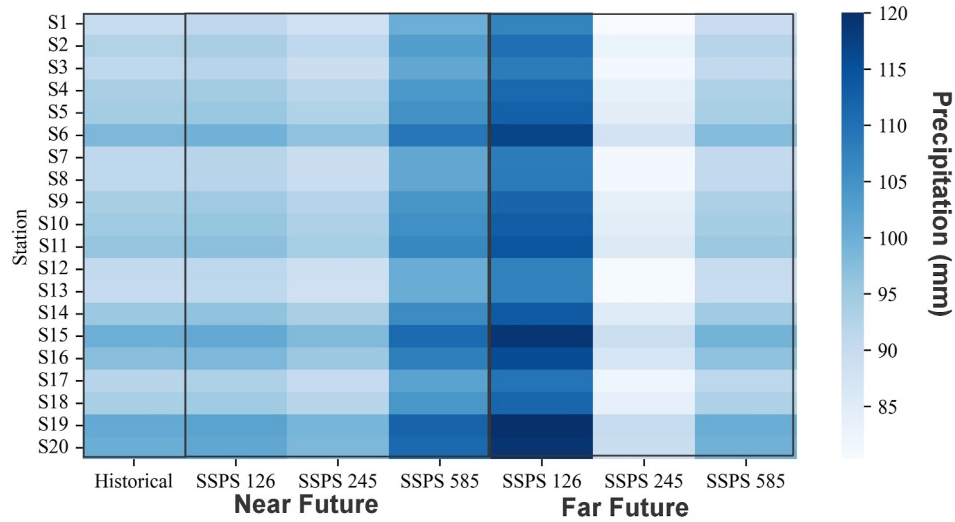

Figure 10. Mean of annual maximum precipitation in historical (1985–2014), near future (2040–2069) and far future (2070–2100) at the weather stations (S1, S2 etc.).

of climate change on regional hydrology, hydroclimatic extremes (e.g., floods and droughts), and water quality using hydrologic, hydrodynamic, and watershed models. Such models guide future planning and management to manage floods, droughts, and water pollution. As the South Florida system includes numerous infrastructures that are operated to provide services like flood management, water supply, and ecosystem protection, the operational rules of these infrastructures can be revisited to adapt to future climate conditions. The need for new alternatives such as new artificial reservoirs (e.g., stormwater treatment areas) can be also explored to better cope with climate change (Jolliffe & Cadima, 2016; Kirwan et al., 2016; Seka et al., 2022). In addition to partitioning the uncertainty of bias correction of climate change into contributions from internal variability, one should consider the climate model response uncertainty and emission scenarios (e.g., SSPs), which they historically relied on making assumptions about forced changes in the mean and variability (Lehner et al., 2020).

We evaluated nine GCMs in this paper and used the best GCM to project future precipitation and air temperature. Previous studies have not been in consensus about the required number of GCMs for climate change impact assessments across South Florida. This remains an open research question to explore in the future.

6. Summary and Conclusions

Transferring GCMs' outputs to local scales requires bias correction. This can be performed using a range of techniques (Rummukainen, 2010; Tabor & Williams, 2010). The main difference between these techniques are assumptions, structure, objectives, and accuracy of outputs as well as their computational costs. SD and dynamical downscaling are two well-known methods to transfer the results of large-scale climate models to the regional and local scales (Ehret et al., 2012; Hawkins et al., 2013). Here, we focused on SD methods. EQM, a specific implementation of quantile mapping that relies on empirical estimates of the quantiles from the climate observations and model simulations.

The outputs of the EQM method at a daily timescale was slightly different from the quantile of observations in extreme parts, presenting distortion in the estimation of extreme precipitation events (Kim et al., 2021). EQM is prone to overfitting and cannot satisfactorily estimate the extreme values. To resolve this issue, we utilized the EQM-LIN method, as a hybrid bias correction approach, to increase the accuracy of the estimated upper quantiles. The performance of EQM-LIN was evaluated across South Florida, a complex managed coastal system that has experienced extreme climatic and weather hazards.

The performance of EQM and EQM-LIN was compared for nine GCMs and three climate variables—precipitation and maximum and minimum air temperatures—at ~20 weather stations. The results confirmed the superior performance of EQM-LIN method in bias correcting GCMs. At the majority of stations, BCC-CSM2-MR outperformed the other GCMs in predicting the three climate variables. The improvement in the bias correction of

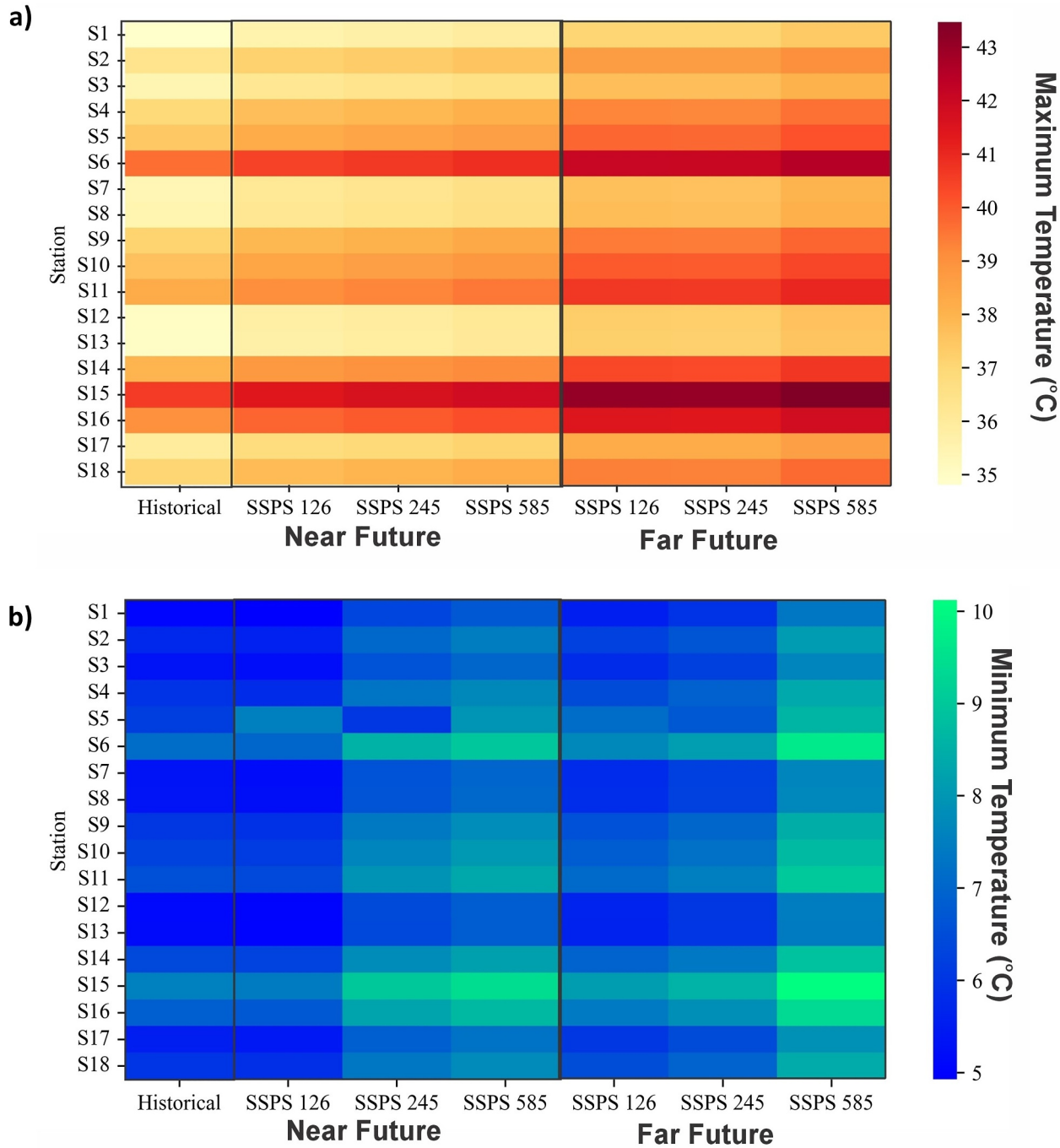

Figure 11. (a) Mean of annual maximum of maximum temperature and (b) Mean of annual maximum of minimum temperature in historical (1985–2014), near future (2040–2069) and far future (2070–2100) at the weather stations (S1, S2 etc.).

daily precipitation by EQM-LIN method was substantial. For instance, at Miami weather station, improvements were up to 70% (according to MAE) and 27% (according to R^2) in May. At the same station, the improvement for daily maximum temperature in August was up to 44% (according to MAE) and 18% (according to R^2).

The importance of extreme precipitation events in the future for South Florida's water management, especially for populated city like Miami, is significant due to the unique environmental, economic, and social challenges facing this region. Hence, choosing a proper approach to project climate variables is critical for designing physical

10.1029/2024EF004531

Figure 12. Percentage of difference in the mean values of annual maximum precipitation estimated by the empirical quantile mapping (EQM) and EQM with linear correction (EQM-LIN) in historical (1985–2014), near future (2040–2069) and far future (2070–2100) at the weather stations.

infrastructures and adapting to the future climate. Since EQM-LIN outperformed EQM in the historical period, especially in the climatic extremes, we compared the ECDFs of daily maximum precipitation in each month using the best GCM under three future scenarios (SSPs 126, 245 and 585) in near future (2040–2069) and far future (2070–2100). The comparisons between the projected precipitation showed that, compared to EQM-LIN, EQM underestimated high quantile of precipitation by up to 26% in near future under SSP585. Such underestimates can lead to inadequate preparation and planning for flood management and climate adaptation. As South Florida already experiences flooding from heavy precipitation events, planning for future climate using inefficient methods like EQM can exacerbate these issue, thereby placing infrastructure and local communities at future risks.

Using the best GCM at each station, the future scenarios (SSPs 126, 245, and 585) were projected using EQM-LIN. At the majority of the weather stations, future projected mean annual maximum of precipitation in near future (2040–2069) and far future (2070–2100), compared to historical period (1985–2014) decreased, but mean of annual maximum of maximum temperature and minimum of temperature increased in both near and far future. The upward trend in temperature underscores the need for revising building, construction, and transportation codes. Additionally, changes in precipitation, though relatively small in this study area, calls for updates to intensity-duration-frequency curves, hazard risk maps, insurance rates, civil infrastructure design (such as levees and canals), and regulatory frameworks governing hydraulic structures like gated spillways. Although there was no statistically significant trend in average annual maximum and minimum air temperature over the historical period, mostly increasing trends were observed in the future scenarios (5% significance level), consistent with previous studies (e.g., NOAA, 2022) based on the ensemble of CMIP5 models; the median of temperature is expected to increase for South Florida. Monthly precipitation at the majority of weather stations exhibited a slight decrease in the summer (June, July, and August), an increase in the fall (October and November), and a slight decrease annually (95% confidence level) under the future scenarios. This finding was also in line with previous studies in the study area (Butcher et al., 2023; Infanti et al., 2020; Obeysekera et al., 2017; USDA, 2024).

While researchers have studied the future climate of South Florida, our work demonstrated the application of a hybrid statistical bias correction approach that improves the prediction of high quantiles (extremes) of precipitation and air temperature. Our comparative analyses suggested that nationally and globally downscaled CMIP6 data tend to underestimate high quantiles of precipitation and are inappropriate for extreme precipitation values. As such, extreme precipitation should be derived using in situ observations and region/local-specific bias

10.1029/2024EF004531

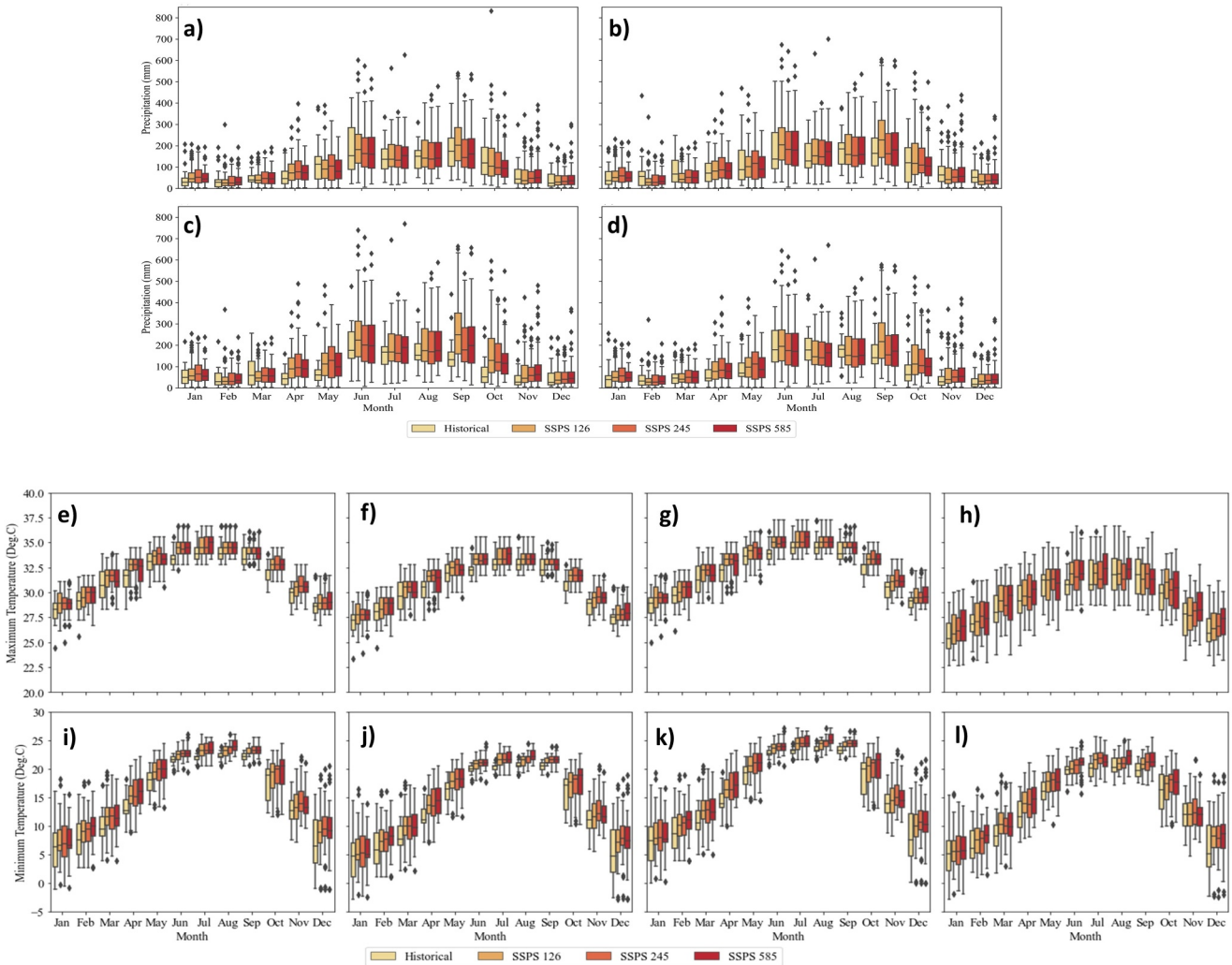

Figure 13. Boxplots of: (Top panel (a–d)) monthly precipitation at: (a) Miami, (b) West Palm Beach, (c) Orlando, and (d) Naples weather stations, and (Bottom panels (e–j)) monthly average of maximum and minimum air temperature at: (e and i) Miami, (f and j) West Palm Beach, (g and k) Orlando and (h and l) Naples weather stations in the historical (1985–2014) and future scenarios (2015–2100).

correction approaches like EQM-LIN. Such coarse scale data may be, however, sufficient for air temperature and low/medium quantiles of precipitation.

The combination of rising temperature with decreasing/increasing precipitating causes a sequence of natural hazards like drought and flooding, which have extensive impacts on all strata of society, from agricultural production to power generation and beyond. The results also suggested that South Florida can be prone to the sequence of drought and flooding from summer to fall in the future, implying the need for designing proper infrastructure to be more compatible with these temporally compound climate and weather events. Our future projections indicated a rise in average annual maximum temperatures, emphasizing the need for proactive ecosystem protection in addition to updating operational codes and human health and safety guidelines. These updates have implications for various state and federal agencies, such as Federal Emergency Management Agency (FEMA), US Army Corps of Engineers (USACE), National Park Service and SFWMD. Overall, our study advocates for the development of climate adaptation plans, particularly for highly managed water systems like South Florida. Our findings also suggest the need to revise irrigation schedules in agricultural areas and the operational rules of regulating hydraulic structures, such as gated spillways, to prioritize ecosystem and population protection. For example, revising the operational rules of gated spillways in Water Conservation Areas can better safeguard the ecosystem of Everglades National Park against future climate anomalies, considering the

10.1029/2024EF004531

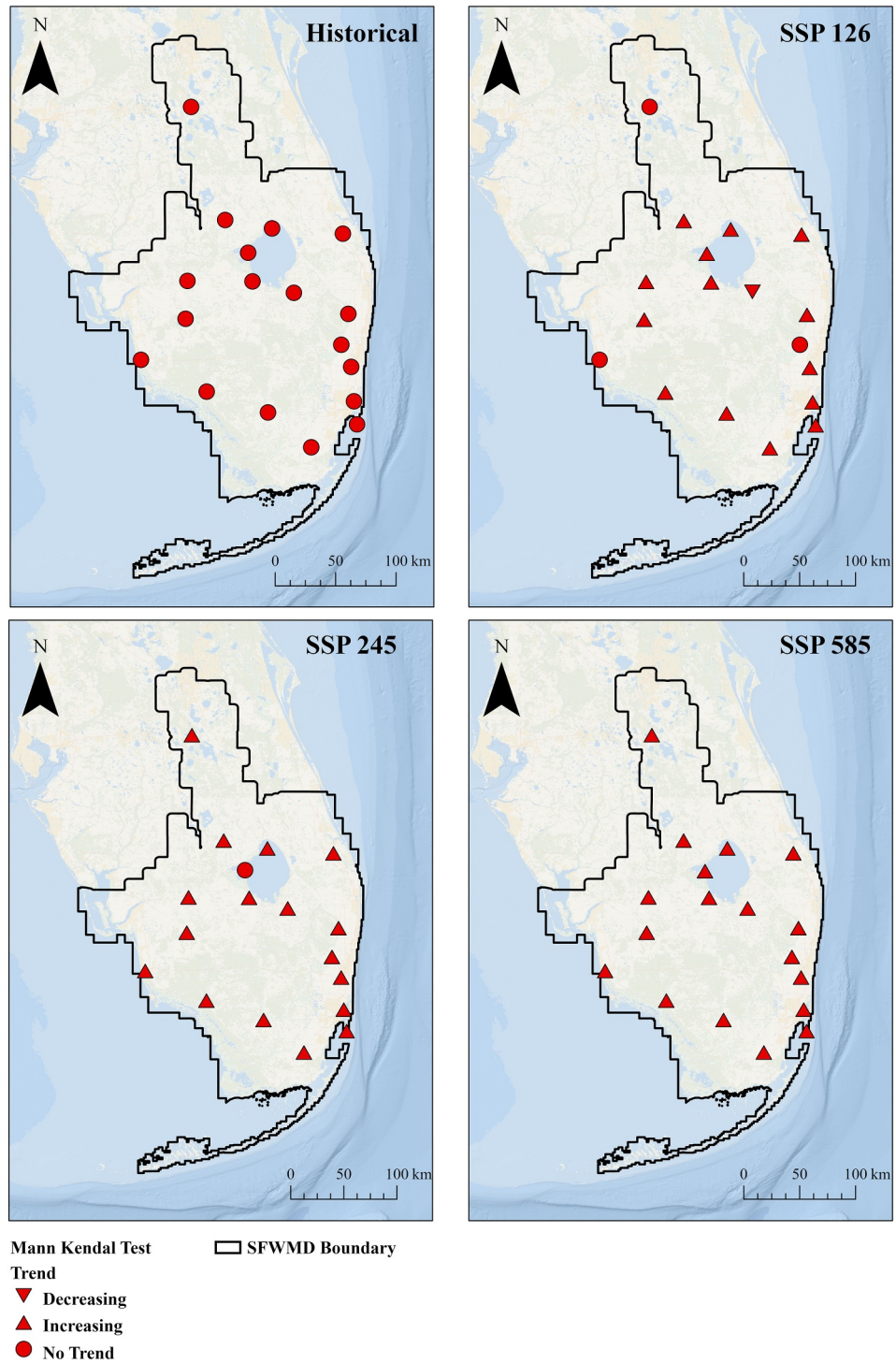

Figure 14. Monotonic trend analyses of annual maximum air temperature in historical (1985–2014) and future scenarios (1985–2100) under three shared socioeconomic pathways at different weather stations across the study area. SFWMD, South Florida Water Management District.

impact of warmer climates on evaporation dynamics. Similarly, adjustments to operational rules around Lake Okeechobee will be necessary to address the effects on agricultural areas, like the Everglades Agricultural Area, and to ensure the proper management of the lake's water levels.

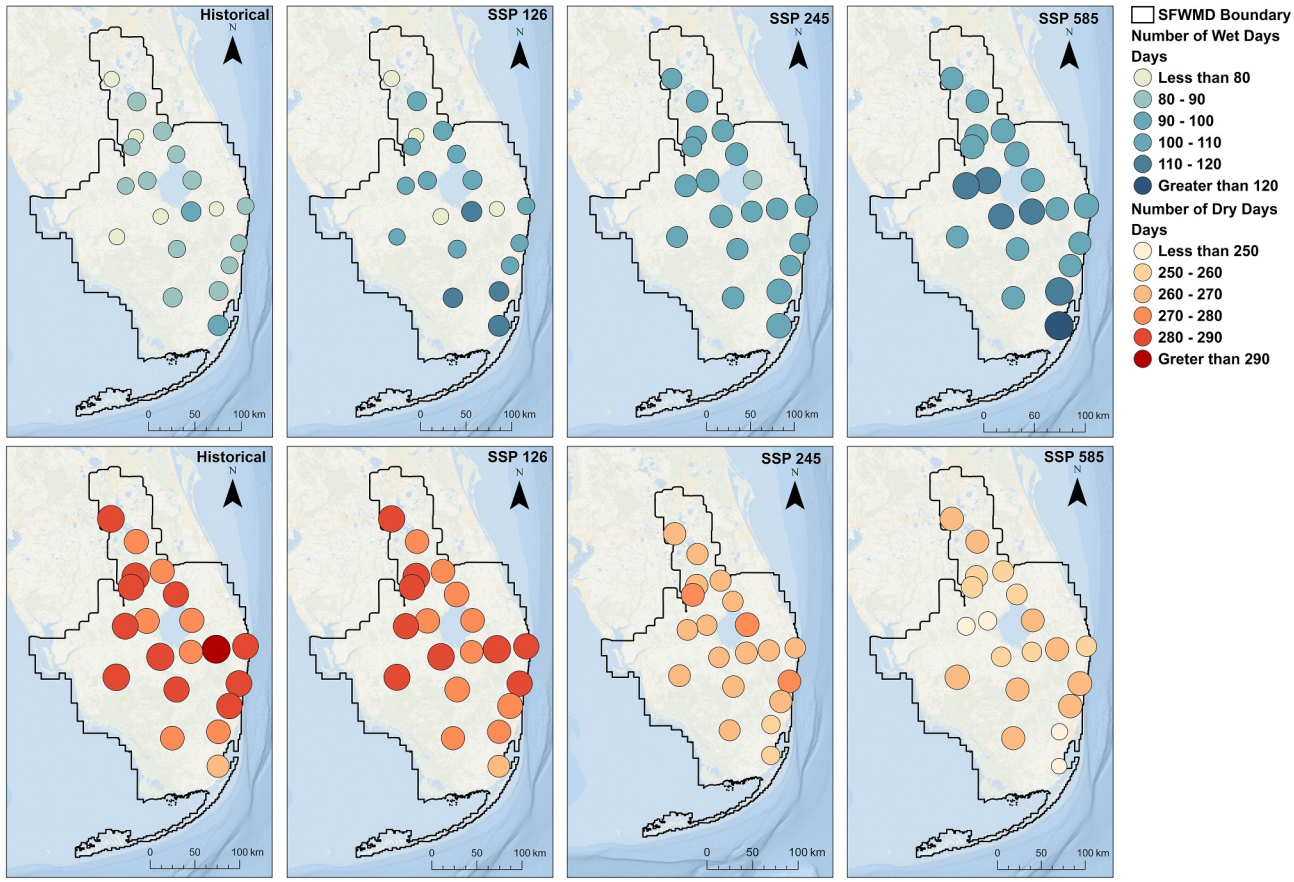

Figure 15. Number of wet days and dry days at weather stations across the study area in the historical and future periods.

Data Availability Statement

Historical precipitation and air temperature data were acquired from SFWMD's DBHYDRO database (SFWMD, 2024) and NOAA's NCEI (NOAA, 2024). Simulated precipitation and air temperature by the GCMs for historical and future climate scenarios were obtained from Earth System Grid Federation (2024). The Oak Ridge National Lab downscaled data are available from Kao et al. (2022).

Acknowledgments
We thank Florida State University's Librararies for partially supporting the open-access fees of this article through the Open Access Publishing Fund.

References

Aditya, F., Gusmayanti, E., & Sudrajat, J. (2021). Rainfall trend analysis using Mann-Kendall and Sen's slope estimator test in West Kalimantan. In *IOP conference series: Earth and environmental science* (Vol. 893, p. 012006). https://doi.org/10.1088/1755-1315/893/1/012006

Akinsanola, A. A., Kooperman, G. J., Reed, K. A., Pendergrass, A. G., & Hannah, W. M. (2020). Projected changes in seasonal precipitation extremes over the United States in CMIP6 simulations. *Environmental Research Letters*, *15*(10), 104078. https://doi.org/10.1088/1748-9326/abb397

Alizadeh-Choobari, O., & Najafi, M. S. (2018). Climate variability in Iran in response to the diversity of the El Niño-Southern Oscillation. *International Journal of Climatology*, *38*(11), 4239–4250. https://doi.org/10.1002/joc.5564

Almazroui, M., Islam, M. N., Saeed, F., Saeed, S., Ismail, M., Ehsan, M. A., et al. (2021). Projected changes in temperature and precipitation over the United States, Central America, and the Caribbean in CMIP6 GCMs. *Earth Systems and Environment*, *5*(1), 1–24. https://doi.org/10.1007/s41748-021-00199-5

Araya-Osses, D., Casanueva, A., Román-Figueroa, C., Uribe, J. M., & Paneque, M. (2020). Climate change projections of temperature and precipitation in Chile based on statistical downscaling. *Climate Dynamics*, *54*(9–10), 4309–4330. https://doi.org/10.1007/s00382-020-05231-4

Arnell, N. W., & Gosling, S. N. (2015). The impacts of climate change on river flood risk at the global scale. *Climatic Change*, *134*(3), 387–401. https://doi.org/10.1007/s10584-014-1084-5

Ashfaq, M., Rastogi, D., Kitson, J., Abid, M. A., & Kao, S.-C. (2022). Evaluation of CMIP6 GCMS over the conus for downscaling studies. *Journal of Geophysical Research: Atmospheres*, *127*(21), e2022JD036659. https://doi.org/10.1029/2022jd036659

Bates, P. D., Quinn, N., Sampson, C., Smith, A., Wing, O., Sosa, J., et al. (2021). Combined modeling of US fluvial, pluvial, and coastal flood hazard under current and future climates. *Water Resources Research*, *57*(2), e2020WR028673. https://doi.org/10.1029/2020wr028673

Bayissa, Y., Melesse, A., Bhat, M., Tadesse, T., & Shiferaw, A. (2021). Evaluation of regional climate models (RCMs) using precipitation and temperature-based climatic indices: A case study of Florida, USA. *Water*, *13*(17), 2411. https://doi.org/10.3390/w13172411

Bettolli, M. L. (2021). Analog models for empirical-statistical downscaling. https://doi.org/10.1093/acrefore/9780190228620.013.738
Boé, J., Terray, L., Habets, F., & Martin, E. (2006). A simple statistical-dynamical downscaling scheme based on weather types and conditional resampling. *Journal of Geophysical Research*, *111*(D23), D23106. https://doi.org/10.1029/2005jd006889
Boé, J., Terray, L., Habets, F., & Martin, E. (2007). Statistical and dynamical downscaling of the seine basin climate for hydro-meteorological studies. *International Journal of Climatology*, *27*(12), 1643–1655. https://doi.org/10.1002/joc.1602
Broucke, S. V., Wouters, H., Demuzere, M., & van Lipzig, N. P. M. (2018). The influence of convection-permitting regional climate modeling on future projections of extreme precipitation: Dependency on topography and timescale. *Climate Dynamics*, *52*(9–10), 5303–5324. https://doi.org/10.1007/s00382-018-4454-2
Butcher, J. B., Sarkar, S., Johnson, T. E., & Shabani, A. (2023). Spatial analysis of future climate risk to stormwater infrastructure. *JAWRA Journal of the American Water Resources Association*, *59*(6), 1383–1396. https://doi.org/10.1111/1752-1688.13132
Camus, P., Menéndez, M., Méndez, F. J., Izaguirre, C., Espejo, A., Cánovas, V., et al. (2014). A weather-type statistical downscaling framework for ocean wave climate. *Journal of Geophysical Research: Oceans*, *119*(11), 7389–7405. https://doi.org/10.1002/2014jc010141
Carpenter, T. M., & Georgakakos, K. P. (2001). Assessment of Folsom lake response to historical and potential future climate scenarios: 1. Forecasting. *Journal of Hydrology*, *249*(1–4), 148–175. https://doi.org/10.1016/s0022-1694(01)00417-6
Cook, B. I., Mankin, J. S., & Anchukaitis, K. J. (2018). Climate change and drought: From past to future. *Current Climate Change Reports*, *4*(2), 164–170. https://doi.org/10.1007/s40641-018-0093-2
Dai, A., Zhao, T., & Chen, J. (2018). Climate change and drought: A precipitation and evaporation perspective. *Current Climate Change Reports*, *4*(3), 301–312. https://doi.org/10.1007/s40641-018-0101-6
Danabasoglu, G. (2019). NCAR CESM2 model output prepared for CMIP6 CMIP historical. https://doi.org/10.22033/ESGF/CMIP6.7627
Davini, P., Corti, S., D'Andrea, F., Rivière, G., & von Hardenberg, J. (2017). Improved winter European atmospheric blocking frequencies in high-resolution global climate simulations. *Journal of Advances in Modeling Earth Systems*, *9*(7), 2615–2634. https://doi.org/10.1002/2017MS001082
Dix, M., Bi, D., Dobrohotoff, P., Fiedler, R., Harman, I., Law, R., et al. (2019). CSIRO-ARCCSS ACCESS-CM2 model output prepared for CMIP6 CMIP historical. https://doi.org/10.22033/ESGF/CMIP6.4271
Earth System Grid Federation. (2024). CMIP6 project [Dataset]. Retrieved from https://aims2.llnl.gov/search/cmip6/?institution_id=NCAR&source_id=CESM2&experiment_id=1pctCO2&variant_label=r1i1p1f1
EC-Earth Consortium (EC-Earth). (2019). EC-Earth-consortium EC-Earth3-veg model output prepared for CMIP6 ScenarioMIP. https://doi.org/10.22033/ESGF/CMIP6.727
Ehret, U., Zehe, E., Wulfmeyer, V., Warrach-Sagi, K., & Liebert, J. (2012). Hess opinions "should we apply bias correction to global and regional climate model data"? *Hydrology and Earth System Sciences*, *16*(9), 3391–3404. https://doi.org/10.5194/hess-16-3391-2012
Emori, S., & Brown, S. J. (2005). Dynamic and thermodynamic changes in mean and extreme precipitation under changed climate. *Geophysical Research Letters*, *32*(17), L17706. https://doi.org/10.1029/2005gl023272
Eyring, V., Bony, S., Meehl, G. A., Senior, C. A., Stevens, B., Stouffer, R. J., & Taylor, K. E. (2016). Overview of the coupled model intercomparison project phase 6 (CMIP6) experimental design and organization. *Geoscientific Model Development*, *9*(5), 1937–1958. https://doi.org/10.5194/gmd-9-1937-2016
Fauzi, F., Kuswanto, H., & Atok, R. M. (2020). Bias correction and statistical downscaling of Earth system models using quantile delta mapping (QDM) and bias correction constructed analogues with quantile mapping reordering (BCCAQ). *Journal of Physics: Conference Series*, *1538*(1), 012050. https://doi.org/10.1088/1742-6596/1538/1/012050
Fu, G., Charles, S. P., Chiew, F. H., Ekström, M., & Potter, N. J. (2018). Uncertainties of statistical downscaling from predictor selection: Equifinality and transferability. *Atmospheric Research*, *203*, 130–140. https://doi.org/10.1016/j.atmosres.2017.12.008
Ghanbari, M., Arabi, M., Georgescu, M., & Broadbent, A. M. (2023). The role of climate change and urban development on compound dry-hot extremes across US cities. *Nature Communications*, *14*(1), 3509. https://doi.org/10.1038/s41467-023-39205-x
Gilroy, K. L., & McCuen, R. H. (2012). A nonstationary flood frequency analysis method to adjust for future climate change and urbanization. *Journal of Hydrology*, *414–415*, 40–48. https://doi.org/10.1016/j.jhydrol.2011.10.009
Grillakis, M. G., Koutroulis, A. G., Daliakopoulos, I. N., & Tsanis, I. K. (2017). A method to preserve trends in quantile mapping bias correction of climate modeled temperature. *Earth System Dynamics*, *8*(3), 889–900. https://doi.org/10.5194/esd-8-889-2017
Gudmundsson, L., Bremnes, J. B., Haugen, J. E., & Engen-Skaugen, T. (2012). Technical note: Downscaling RCM precipitation to the station scale using statistical transformations ndash; a comparison of methods. *Hydrology and Earth System Sciences*, *16*(9), 3383–3390. https://doi.org/10.5194/hess-16-3383-2012
Gutowski, W. J., Decker, S. G., Donavon, R. A., Pan, Z., Arritt, R. W., & Takle, E. S. (2003). Temporal–spatial scales of observed and simulated precipitation in central U.S. climate. *Journal of Climate*, *16*(22), 3841–3847. https://doi.org/10.1175/1520-0442(2003)016⟨3841:TSOOAS⟩2.0.CO;2
Hallegatte, S., Green, C., Nicholls, R. J., & Corfee-Morlot, J. (2013). Future flood losses in major coastal cities. *Nature Climate Change*, *3*(9), 802–806. https://doi.org/10.1038/nclimate1979
Han, E., & Ines, A. V. (2017). Downscaling probabilistic seasonal climate forecasts for decision support in agriculture: A comparison of parametric and non-parametric approach. *Climate Risk Management*, *18*, 51–65. https://doi.org/10.1016/j.crm.2017.09.003
Hawkins, E., Osborne, T. M., Ho, C. K., & Challinor, A. J. (2013). Calibration and bias correction of climate projections for crop modelling: An idealised case study over Europe [Agricultural prediction using climate model ensembles]. *Agricultural and Forest Meteorology*, *170*, 19–31. https://doi.org/10.1016/j.agrformet.2012.04.007
Hessami, M., Gachon, P., Ouarda, T. B., & St-Hilaire, A. (2008). Automated regression-based statistical downscaling tool. *Environmental Modelling & Software*, *23*(6), 813–834. https://doi.org/10.1016/j.envsoft.2007.10.004
Hewitson, B. C., Daron, J., Crane, R. G., Zermoglio, M. F., & Jack, C. (2014). Interrogating empirical-statistical downscaling. *Climatic Change*, *122*(4), 539–554. https://doi.org/10.1007/s10584-013-1021-z
Holthuijzen, M., Beckage, B., J.Clemins, P., Higdon, D., & Winter, J. M. (2022). Robust bias-correction of precipitation extremes using a novel hybrid empirical quantile-mapping method. *Theoretical and Applied Climatology*, *149*(1–2), 863–882. https://doi.org/10.1007/s00704-022-04035-2
Holthuijzen, M. F., Beckage, B., Clemins, P. J., Higdon, D., & Winter, J. M. (2021). Constructing high-resolution, bias-corrected climate products: A comparison of methods. *Journal of Applied Meteorology and Climatology*, *60*(4), 455–475. https://doi.org/10.1175/jamc-d-20-0252.1
Infanti, J. M., Kirtman, B. P., Aumen, N. G., Stamm, J., & Polsky, C. (2020). Assessment of uncertainty in multi-model means of downscaled South Florida precipitation for projected (2019–2099) climate. *International Journal of Climatology*, *40*(5), 2764–2777. https://doi.org/10.1002/joc.6365

K. T. Ingram, K. Dow, L. Carter, & J. Anderson (Eds.), (2013). *Climate of the southeast United States*. Island Press/Center for Resource Economics. https://doi.org/10.5822/978-1-61091-509-0

Irizarry-Ortiz, M. M., Stamm, J. F., Maran, C., & Obeysekera, J. (2022). Development of projected depth-duration frequency curves (2050–89) for South Florida. https://doi.org/10.3133/sir20225093

Jebeile, J., Lam, V., & Räz, T. (2020). Understanding climate change with statistical downscaling and machine learning. *Synthese*, *199*(1–2), 1877–1897. https://doi.org/10.1007/s11229-020-02865-z

Jolliffe, I. T., & Cadima, J. (2016). Principal component analysis: A review and recent developments. *Philosophical Transactions of the Royal Society A: Mathematical, Physical & Engineering Sciences*, *374*(2065), 20150202. https://doi.org/10.1098/rsta.2015.0202

Joshi, N., & Kalra, A. (2021). Analyzing the association between ENSO and groundwater rise in the South Atlantic-Gulf Region in the southeastern United States. *Hydrology*, *8*(3), 119. https://doi.org/10.3390/hydrology8030119

Kao, S.-C., Ashfaq, M., Rastogi, D., & Gangrade, S. (2022). The third SECURE water act section 9505 assessment (9505V3) [Dataset]. https://doi.org/10.21951/SWA9505V3/1887469

Keller, D. E., Fischer, A. M., Liniger, M. A., Appenzeller, C., & Knutti, R. (2017). Testing a weather generator for downscaling climate change projections over Switzerland. *International Journal of Climatology*, *37*(2), 928–942. https://doi.org/10.1002/joc.4750

Kim, S., Joo, K., Kim, H., Shin, J.-Y., & Heo, J.-H. (2021). Regional quantile delta mapping method using regional frequency analysis for regional climate model precipitation. *Journal of Hydrology*, *596*, 125685. https://doi.org/10.1016/j.jhydrol.2020.125685

Kirtman, B., Misra, V., Burgman, R., Infanti, J., & Obeysekera, J. (2017). Florida climate variability and prediction. In *Florida's climate: Changes, variations, & impacts*. Florida Climate Institute. https://doi.org/10.17125/fci2017.ch17

Kirwan, M. L., Temmerman, S., Skeehan, E. E., Guntenspergen, G. R., & Fagherazzi, S. (2016). Overestimation of marsh vulnerability to sea level rise. *Nature Climate Change*, *6*(3), 253–260. https://doi.org/10.1038/nclimate2909

Kröner, N., Kotlarski, S., Fischer, E., Lüthi, D., Zubler, E., & Schär, C. (2016). Separating climate change signals into thermodynamic, lapse-rate and circulation effects: Theory and application to the European summer climate. *Climate Dynamics*, *48*(9–10), 3425–3440. https://doi.org/10.1007/s00382-016-3276-3

Kulp, S., & Strauss, B. H. (2017). Rapid escalation of coastal flood exposure in US municipalities from sea level rise. *Climatic Change*, *142*(3–4), 477–489. https://doi.org/10.1007/s10584-017-1963-7

Lafon, T., Dadson, S., Buys, G., & Prudhomme, C. (2013). Bias correction of daily precipitation simulated by a regional climate model: A comparison of methods. *International Journal of Climatology*, *33*(6), 1367–1381. https://doi.org/10.1002/joc.3518

Lanzante, J. R., Dixon, K. W., Nath, M. J., Whitlock, C. E., & Adams-Smith, D. (2018). Some pitfalls in statistical downscaling of future climate. *Bulletin of the American Meteorological Society*, *99*(4), 791–803. https://doi.org/10.1175/bams-d-17-0046.1

Latif, M. (2011). Uncertainty in climate change projections. *Journal of Geochemical Exploration*, *110*(1), 1–7. https://doi.org/10.1016/j.gexplo.2010.09.011

Legasa, M. N., Thao, S., Vrac, M., & Manzanas, R. (2023). Assessing three perfect prognosis methods for statistical downscaling of climate change precipitation scenarios. *Geophysical Research Letters*, *50*(9), e2022GL102525. https://doi.org/10.1029/2022GL102525

Lehner, F., Deser, C., Maher, N., Marotzke, J., Fischer, E. M., Brunner, L., et al. (2020). Partitioning climate projection uncertainty with multiple large ensembles and CMIP5/6. *Earth System Dynamics*, *11*(2), 491–508. https://doi.org/10.5194/esd-11-491-2020

Levene, H. (1960). Robust tests for equality of variances. In I. Olkin, S. G. Ghuye, W. Hoeffding, W. G. Madow, & H. B. Mann (Eds.), *Contributions to probability and statistics: Essays in honor of Harold Hotelling*. Stanford University Press.

Lim, Y.-K., Shin, D. W., Cocke, S., LaRow, T. E., Schoof, J. T., O'Brien, J. J., & Chassignet, E. P. (2007). Dynamically and statistically downscaled seasonal simulations of maximum surface air temperature over the southeastern United States. *Journal of Geophysical Research*, *112*(D24), D24102. https://doi.org/10.1029/2007jd008764

Maraun, D., & Widmann, M. (2017). *Statistical downscaling and bias correction for climate research*. Cambridge University Press. https://doi.org/10.1017/9781107588783

Massey, F. J. (1951). The Kolmogorov-Smirnov test for goodness of fit. *Journal of the American Statistical Association*, *46*(253), 68–78. https://doi.org/10.1080/01621459.1951.10500769

Mauritsen, T., Bader, J., Becker, T., Behrens, J., Bittner, M., Brokopf, R., et al. (2019). Developments in the MPI-M Earth system model version 1.2 (MPI-ESM1.2) and its response to increasing CO_2. *Journal of Advances in Modeling Earth Systems*, *11*(4), 998–1038. https://doi.org/10.1029/2018ms001400

Mayou, L. A., Alamdari, N., Ahmadisharaf, E., & Kamali, M. (2024). Impacts of future climate and land use/land cover change on urban runoff using fine-scale hydrologic modeling. *Journal of Environmental Management*, *362*, 121284. https://doi.org/10.1016/j.jenvman.2024.121284

McBride, L. A., Hope, A. P., Canty, T. P., Bennett, B. F., Tribett, W. R., & Salawitch, R. J. (2021). Comparison of CMIP6 historical climate simulations and future projected warming to an empirical model of global climate. *Earth System Dynamics*, *12*(2), 545–579. https://doi.org/10.5194/esd-12-545-2021

Mearns, L. O., Sain, S., Leung, L. R., Bukovsky, M. S., McGinnis, S., Biner, S., et al. (2013). Climate change projections of the North American regional climate change assessment program (NARCCAP). *Climatic Change*, *120*(4), 965–975. https://doi.org/10.1007/s10584-013-0831-3

Mendoza Paz, S., & Willems, P. (2022). Uncovering the strengths and weaknesses of an ensemble of quantile mapping methods for downscaling precipitation change in southern Africa. *Journal of Hydrology: Regional Studies*, *41*, 101104. https://doi.org/10.1016/j.ejrh.2022.101104

Mishra, V., Bhatia, U., & Tiwari, A. D. (2020). Bias-corrected climate projections for South Asia from coupled model intercomparison project-6. *Scientific Data*, *7*(1), 338. https://doi.org/10.1038/s41597-020-00681-1

Misra, V., Carlson, E., Craig, R. K., Enfield, D., Kirtman, B., Landing, W., et al. (2011). Climate scenarios: A Florida-centric view, Florida climate change task force. *State University System of Florida*. http://floridaclimate.org/whitepapers/

Misra, V., Mishra, A., & Bhardwaj, A. (2019). A coupled ocean-atmosphere downscaled climate projection for the peninsular Florida region. *Journal of Marine Systems*, *194*, 25–40. https://doi.org/10.1016/j.jmarsys.2019.02.010

Mukherjee, S., Mishra, A., & Trenberth, K. E. (2018). Climate change and drought: A perspective on drought indices. *Current Climate Change Reports*, *4*(2), 145–163. https://doi.org/10.1007/s40641-018-0098-x

National Academies of Sciences, E., & Medicine. (2022). *Progress toward restoring the everglades: The ninth biennial review—2022*. The National Academies Press. https://doi.org/10.17226/26706

Naumann, G., Cammalleri, C., Mentaschi, L., & Feyen, L. (2021). Increased economic drought impacts in Europe with anthropogenic warming. *Nature Climate Change*, *11*(6), 485–491. https://doi.org/10.1038/s41558-021-01044-3

NOAA. (2022). *National oceanic and atmospheric administration [NOAA], Physical Sciences Laboratory—NOAA's climate change web portal: NOAA database*. NOAA. Retrieved from https://psl.noaa.gov/ipcc/cmip5/maps.html

NOAA. (2024). National Centers for Environmental Information [Dataset]. Retrieved from https://www.ncei.noaa.gov/cdo-web/search;jsessionid=DCFB5ACC4BB28B6581B3355CA2B1C869

Nourani, V., Razzaghzadeh, Z., Baghanam, A. H., & Molajou, A. (2019). ANN-based statistical downscaling of climatic parameters using decision tree predictor screening method. *Theoretical and Applied Climatology*, *137*(3–4), 1729–1746. https://doi.org/10.1007/s00704-018-2686-z

Obeysekera, J., Graham, W., Sukop, M., Asefa, T., Wang, D., Ghebremichael, K., & Mwashote, B. (2017). Implications of climate change on Florida's water resources. In *Florida's climate: Changes, variations, & impacts*. Florida Climate Institute. https://doi.org/10.17125/fci2017.ch03

O'Gorman, P. A. (2015). Precipitation extremes under climate change. *Current Climate Change Reports*, *1*(2), 49–59. https://doi.org/10.1007/s40641-015-0009-3

Panofsky, H. (1968). *Some applications of statistics to meteorology; Earth and mineral sciences continuing education, college of Earth and mineral sciences*. Pennsylvania State University.

Piani, C., Haerter, J. O., & Coppola, E. (2010). Statistical bias correction for daily precipitation in regional climate models over Europe. *Theoretical and Applied Climatology*, *99*(1–2), 187–192. https://doi.org/10.1007/s00704-009-0134-9

Polade, S. D., Pierce, D. W., Cayan, D. R., Gershunov, A., & Dettinger, M. D. (2014). The key role of dry days in changing regional climate and precipitation regimes. *Scientific Reports*, *4*(1), 4364. https://doi.org/10.1038/srep04364

Rastogi, D., Kao, S.-C., & Ashfaq, M. (2022). How may the choice of downscaling techniques and meteorological reference observations affect future hydroclimate projections? *Earth's Future*, *10*(8). https://doi.org/10.1029/2022ef002734

Rummukainen, M. (2010). State-of-the-art with regional climate models. *WIREs Climate Change*, *1*(1), 82–96. https://doi.org/10.1002/wcc.8

Sachindra, D. A., Ahmed, K., Shahid, S., & Perera, B. J. C. (2018). Cautionary note on the use of genetic programming in statistical downscaling. *International Journal of Climatology*, *38*(8), 3449–3465. https://doi.org/10.1002/joc.5508

Sangelantoni, L., Russo, A., & Gennaretti, F. (2019). Impact of bias correction and downscaling through quantile mapping on simulated climate change signal: A case study over central Italy. *Theoretical and Applied Climatology*, *135*(1–2), 725–740. https://doi.org/10.1007/s00704-018-2406-8

Santos, J. A., Belo-Pereira, M., Fraga, H., & Pinto, J. G. (2016). Understanding climate change projections for precipitation over western Europe with a weather typing approach. *Journal of Geophysical Research: Atmospheres*, *121*(3), 1170–1189. https://doi.org/10.1002/2015JD024399

Schiermeier, Q. (2018). Droughts, heatwaves and floods: How to tell when climate change is to blame. *Nature*, *560*(7716), 20–22. https://doi.org/10.1038/d41586-018-05849-9

Schoof, J. T. (2013). Statistical downscaling in climatology. *Geography Compass*, *7*(4), 249–265. https://doi.org/10.1111/gec3.12036

Schoof, J. T., & Pryor, S. C. (2001). Downscaling temperature and precipitation: A comparison of regression-based methods and artificial neural networks. *International Journal of Climatology*, *21*(7), 773–790. https://doi.org/10.1002/joc.655

Seferian, R. (2018). CNRM-CERFACS CNRM-ESM2-1 model output prepared for CMIP6 CMIP historical. https://doi.org/10.22033/ESGF/CMIP6.4068

Seka, A. M., Zhang, J., Ayele, G. T., Demeke, Y. G., Han, J., & Prodhan, F. A. (2022). Spatio-temporal analysis of water storage variation and temporal correlations in the East Africa lake basins. *Journal of Hydrology: Regional Studies*, *41*, 101094. https://doi.org/10.1016/j.ejrh.2022.101094

Seland, Ø., Bentsen, M., Olivié, D., Toniazzo, T., Gjermundsen, A., Graff, L. S., et al. (2020). Overview of the Norwegian Earth system model (NorESM2) and key climate response of CMIP6 DECK, historical, and scenario simulations. *Geoscientific Model Development*, *13*(12), 6165–6200. https://doi.org/10.5194/gmd-13-6165-2020

SFWMD. (2024). DBHYDRO (Environmental data) [Dataset]. Retrieved from https://my.sfwmd.gov/dbhydroplsql/show_dbkey_info.main_menu

Shamir, E., Halper, E., Modrick, T., Georgakakos, K. P., Chang, H.-I., Lahmers, T. M., & Castro, C. (2019). Statistical and dynamical downscaling impact on projected hydrologic assessment in arid environment: A case study from Bill Williams River basin and Alamo Lake, Arizona. *Journal of Hydrology X*, *2*, 100019. https://doi.org/10.1016/j.hydroa.2019.100019

Shen, Z., Zhang, Q., Singh, V. P., Sun, P., He, C., & Cheng, C. (2021). Station-based non-linear regression downscaling approach: A new monthly precipitation downscaling technique. *International Journal of Climatology*, *41*(13), 5879–5898. https://doi.org/10.1002/joc.7158

Siabi, E. K., Awafo, E. A., Kabo-bah, A. T., Derkyi, N. S. A., Akpoti, K., Mortey, E. M., & Yazdanie, M. (2023). Assessment of shared socioeconomic pathway (SSP) climate scenarios and its impacts on the Greater Accra region. *Urban Climate*, *49*, 101432. https://doi.org/10.1016/j.uclim.2023.101432

Song, J.-H., Her, Y., Shin, S., Cho, J., Paudel, R., Khare, Y. P., et al. (2020). Evaluating the performance of climate models in reproducing the hydrological characteristics of rainfall events. *Hydrological Sciences Journal*, *65*(9), 1490–1511. https://doi.org/10.1080/02626667.2020.1750616

Srivastava, A., Grotjahn, R., & Ullrich, P. A. (2020). Evaluation of historical CMIP6 model simulations of extreme precipitation over contiguous us regions. *Weather and Climate Extremes*, *29*, 100268. https://doi.org/10.1016/j.wace.2020.100268

Srivastava, A., Grotjahn, R., Ullrich, P. A., & Zarzycki, C. (2021). Evaluation of precipitation indices in suites of dynamically and statistically downscaled regional climate models over Florida. *Climate Dynamics*, *58*(5–6), 1587–1611. https://doi.org/10.1007/s00382-021-05980-w

Stocker, T. F., Qin, D.-H., Plattner, G.-K., Tignor, M. M., Allen, S. K., Boschung, J., et al. (2013). Climate change 2013. The physical science basis. Working group I contribution to the fifth assessment report of the intergovernmental panel on climate change—Abstract for decision-makers.

Sunyer, M. A., Hundecha, Y., Lawrence, D., Madsen, H., Willems, P., Martinkova, M., et al. (2015). Inter-comparison of statistical downscaling methods for projection of extreme precipitation in Europe. *Hydrology and Earth System Sciences*, *19*(4), 1827–1847. https://doi.org/10.5194/hess-19-1827-2015

Swart, N. C., Cole, J. N., Kharin, V. V., Lazare, M., Scinocca, J. F., Gillett, N. P., et al. (2019). CCCma CanESM5 model output prepared for CMIP6 ScenarioMIP SSP126. https://doi.org/10.22033/ESGF/CMIP6.3683

Tabor, K., & Williams, J. W. (2010). Globally downscaled climate projections for assessing the conservation impacts of climate change. *Ecological Applications*, *20*(2), 554–565. https://doi.org/10.1890/09-0173.1

Tani, S., & Gobiet, A. (2019). Quantile mapping for improving precipitation extremes from regional climate models. *Journal of Agrometeorology*, *21*(4), 434–443.

Themeßl, M. J., Gobiet, A., & Heinrich, G. (2012). Empirical-statistical downscaling and error correction of regional climate models and its impact on the climate change signal. *Climatic Change*, *112*(2), 449–468. https://doi.org/10.1007/s10584-011-0224-4

Themeßl, M. J., Gobiet, A., & Leuprecht, A. (2011). Empirical-statistical downscaling and error correction of daily precipitation from regional climate models. *International Journal of Climatology*, *31*(10), 1530–1544. https://doi.org/10.1002/joc.2168

Thornton, M., Shrestha, R., Wei, Y., Thornton, P., & Kao, S.-C. (2022). Daymet: Daily surface weather data on a 1-km grid for North America, version 4 r1. https://doi.org/10.3334/ORNLDAAC/2129

Thrasher, B., Wang, W., Michaelis, A., Melton, F., Lee, T., & Nemani, R. (2022). NASA global daily downscaled projections, CMIP6. *Scientific Data*, *9*(1), 262. https://doi.org/10.1038/s41597-022-01393-4

Trenberth, K. (2011). Changes in precipitation with climate change. *Climate Research*, *47*(1), 123–138. https://doi.org/10.3354/cr00953

USDA. (2024). USDA. Retrieved from https://www.climatehubs.usda.gov/sites/default/files/SE%20Climate%20Factsheet.pdf

Uytven, E. V., & Willems, P. (2018). Greenhouse gas scenario sensitivity and uncertainties in precipitation projections for central Belgium. *Journal of Hydrology*, *558*, 9–19. https://doi.org/10.1016/j.jhydrol.2018.01.018

Van Uytven, E., De Niel, J., & Willems, P. (2020). Uncovering the shortcomings of a weather typing method. *Hydrology and Earth System Sciences*, *24*(5), 2671–2686. https://doi.org/10.5194/hess-24-2671-2020

Volk, M., Hoctor, T., Nettles, B., Hilsenbeck, R., & Putz, F. (2017). Florida land use and land cover change in the past 100 years. In *Florida's climate: Changes, variations, & impacts*. Florida Climate Institute. https://doi.org/10.17125/fci2017.ch02

Walton, D., Berg, N., Pierce, D., Maurer, E., Hall, A., Lin, Y.-H., et al. (2020). Understanding differences in California climate projections produced by dynamical and statistical downscaling. *Journal of Geophysical Research: Atmospheres*, *125*(19), e2020JD032812. https://doi.org/10.1029/2020JD032812

Wang, Y., Sivandran, G., & Bielicki, J. M. (2018). The stationarity of two statistical downscaling methods for precipitation under different choices of cross-validation periods. *International Journal of Climatology*, *38*(S1), e330–e348. https://doi.org/10.1002/joc.5375

Wilby, R. L., Wigley, T. M. L., Conway, D., Jones, P. D., Hewitson, B. C., Main, J., & Wilks, D. S. (1998). Statistical downscaling of general circulation model output: A comparison of methods. *Water Resources Research*, *34*(11), 2995–3008. https://doi.org/10.1029/98wr02577

Wilcoxon, F. (1945). Individual comparisons by ranking methods. *Biometric Bulletin*, *1*(6), 80. https://doi.org/10.2307/3001968

Wing, O. E. J., Bates, P. D., Smith, A. M., Sampson, C. C., Johnson, K. A., Fargione, J., & Morefield, P. (2018). Estimates of present and future flood risk in the conterminous United States. *Environmental Research Letters*, *13*(3), 034023. https://doi.org/10.1088/1748-9326/aaac65

Wu, T., Chu, M., Dong, M., Fang, Y., Jie, W., Li, J., et al. (2018). BCC BCC-CSM2MR model output prepared for CMIP6 CMIP historical. https://doi.org/10.22033/ESGF/CMIP6.2948

Xu, Z., Han, Y., Tam, C.-Y., Yang, Z.-L., & Fu, C. (2021). Bias-corrected CMIP6 global dataset for dynamical downscaling of the historical and future climate (1979–2100). *Scientific Data*, *8*(1), 293. https://doi.org/10.1038/s41597-021-01079-3

Yang, Y., Tang, J., Xiong, Z., Wang, S., & Yuan, J. (2019). An intercomparison of multiple statistical downscaling methods for daily precipitation and temperature over China: Present climate evaluations. *Climate Dynamics*, *53*(7–8), 4629–4649. https://doi.org/10.1007/s00382-019-04809-x

Yukimoto, S., Kawai, H., Koshiro, T., Oshima, N., Yoshida, K., Urakawa, S., et al. (2019). The meteorological research institute Earth system model version 2.0, MRI-ESM2.0: Description and basic evaluation of the physical component. *Journal of the Meteorological Society of Japan. Series II*, *97*(5), 931–965. https://doi.org/10.2151/jmsj.2019-051

Zhang, L., Xu, Y., Meng, C., Li, X., Liu, H., & Wang, C. (2020). Comparison of statistical and dynamic downscaling techniques in generating high-resolution temperatures in China from CMIP5 GCMs. *Journal of Applied Meteorology and Climatology*, *59*(2), 207–235. https://doi.org/10.1175/JAMC-D-19-0048.1

Zhang, Y. (2012). Will natural disasters accelerate neighborhood decline? A discrete-time hazard analysis of residential property vacancy and abandonment before and after Hurricane Andrew in Miami-Dade County (1991–2000). *Environment and Planning B: Planning and Design*, *39*(6), 1084–1104. https://doi.org/10.1068/b37121

Zhou, W., Leung, L. R., & Lu, J. (2022). Linking large-scale double-ITCZ bias to local-scale drizzling bias in climate models. *Journal of Climate*, *35*(24), 7965–7979. https://doi.org/10.1175/jcli-d-22-0336.1